DETERMINATION OF LOCAL WIND ENERGY POTENTIALS USING CLIMATE MODELING

by

Kamil ÇÖLLÜ

B.S., Physics Teaching, Karadeniz Technical University, 2010

Submitted to the Institute for Graduate Studies in
Science and Engineering in partial fulfillment of
the requirements for the degree of
Master of Science

Graduate Program in Computational Science and Engineering

Boğaziçi University

2016

ACKNOWLEDGEMENTS

I would like to describe my profound thanks to my supervisor, Prof. M. Levent Kurnaz, whose supportive and instructive behavior to me and my friends in IklimBU. I owe my deepest thanks for his contribution to my education life and his guidance to my life experience. I am very thankful for having the chance of working with him.

In addition, I would like to thank the rest of my thesis committee, Assoc. Prof. Osman Börekçi and Assist. Prof. Tuğba Öztürk for their valuable time, insightful remarks and criticisms.

I would also like to thank my friends Nazan An, M. Tufan Turp, Büşra Bozoğlu, Sibel Saygılı, Eda Aydın Oktay, Çağla Fadıllıoğlu, İhsan Çağatay Kıyısüren, Mustafa Çelebi, Neda Soydan and Duygu Zaptiye for their support and friendship.

I am very grateful and would like to thank my family for their encouragement, for unconditionally supporting me and for being the source of my motivation.

ABSTRACT

DETERMINATION OF LOCAL WIND ENERGY POTENTIALS USING CLIMATE MODELING

After the industrial revolution, the needs of coal and other fossil fuels has been increasing day by day. Intensive burning of fossil fuels has resulted in a rise in the atmospheric CO_2 concentration. In the 18th century, the amount of CO_2 in the atmosphere was almost 280 ppm and now this value is more than 400 ppm. As a result of that, climate is changing rapidly and predicting the climate and its variables, such as wind speed and direction, is more difficult than before.

It is more important to use renewable energy to reduce CO_2 emission to the atmosphere. To be able to do, wind energy is a good option and it is a rising star in the renewable energy market. Determining location of wind power plant according to wind direction and wind speed of region is vital for market.

In order to solve these kinds of problems, an alternative method is applied in this study. To predict wind direction and speed according to the climate change, firstly, I used RegCM4, one of Regional Climate Model version of The Abdus Salam International Centre for Theoretical Physics (ICTP), which is developed in ICTP, for simulating the climate variables and, then I used an open source software Winds on Critical Streamline Surfaces (WOCSS), which is developed by Dr. Francis L. Ludwig, for projecting the wind direction and speed.

The result of this study shows wind speed will increase at the Canakkale Biga region at the future.

ÖZET

İKLİM MODELLEME KULLANILARAK YEREL RÜZGAR ENERJİSİ POTANSİYELİ BELİRLENMESİ

Sanayi devriminden sonra kömür ve fosil yakıtlara olan ihtiyaç günden güne arttı.Fosil yakıtların yoğun kullanılmasının sonucu, atmosferdeki CO_2 konsantrasyonu artmıştır. 18. yüzyılda atmosferdeki CO_2 miktarı yaklaşık 280 ppm'di ve şimdi ise bu miktar 400 ppm'den daha fazladır. Bunun sonucunda, iklim hızla değişmekte ve iklimi ve rüzgar hızı ve yönü gibi değişkenlerini önceden tahmin etmek öncekinden daha zor olmaktadır.

Atmosfere CO_2 salımını azaltmak için yenilenebilir enerjiyi kullanmak daha da önemlidir. Bunu yapabilmek için rüzgar enerjisi iyi bir seçenektir ve rüzgar enerjisi yenilenebilir enerji pazarının yükselen yıldızıdır. Pazar için, bölgenin rüzgar yönü ve hızına bağlı rüzgar enerji santralinin yerinin tesbiti hayati önemdedir.

Bu çalışmada, bu tarz problemlerin çözümü için alternatif bir method uygulanmıştır. İklim değişikliğine bağlı olarak rüzgarın yönünü ve hızını tahmin etmek için, ilk olarak, Abdus Salam Uluslararası Teorik Fizik Merkezi (ICTP)'nin bölgesel iklim modeli olan ve ICTP'de geliştirilen RegCM4'i iklim değişkenlerini modellemek için kullandım ve sonra, rüzgar yönünü ve hızını tahmin etmek için Dr. Francis L. Ludwig tarafından geliştirilen, açık kaynak kodlu olan Kritik Aerodinamik Yüzeylerde Rüzgar (WOCSS) programını kullandım.

Bu çalışmanın sonucu, Canakkale Biga bölgesinde rüzgar hızının gelecekte artacağını göstermektedir.

TABLE OF CONTENTS

LIST OF FIGURES

LIST OF TABLES

LIST OF ACRONYMS/ABBREVIATIONS

AR4	IPCC Fourth Assessment Report, 2007
AR5	IPCC Fifth Assessment Report, 2014
CDO	Climate Data Operators
CO_2	Carbondioxide
COAMPS	Coupled Ocean/Atmosphere Mesoscale Prediction System
ESP	Earth System Physics
GCM	General Circulation Model
GrADS	Grid Analysis and Display System
GRIB	General Regularly-distributed Information in Binary form
HDF	Hierarchical Data Format
ICTP	The Abdus Salam International Centre for Theoretical Physics
IPCC	The Intergovernmental Panel on Climate Change
MPI	Max Planck Institute
NCAR	National Center for Atmospheric Research
NWP	Numerical Weather Prediction
ppm	parts per million
RCM	Regional Climate Model
RCP	Representative Concentration Pathways
RegCM4	Regional Climate Modeling 4
RF	Reference
SRES	Special Report on Emissions Scenarios
UNEP	United Nations Environment Programme
UTM	Universal Transverse Mercator
WMO	World Meteorological Organization
WOCSS	Winds on Critical Streamline Services
WWEA	World Wind Energy Association

1. INTRODUCTION

Due to the climate change, renewable energy resources, such as wind power plants, gain more importance. On the other hand, difficulty of predicting wind patterns, it is a well-known dilemma that the determination of the location of the wind power plants. This question is asked to get more efficiency from the wind power plants; where we shall construct a wind power plant.

In Turkey, there are 4718 MW installed wind energy by end of 2015 and Turkey is the fifteenth of the list of the Wind Energy Worldwide [1].

Table 1.1 gives us hope to reduce the emission of CO_2 and it is the forerunner of the new installments of new wind power plants. Because the wind power is the trending player of the energy market, the question which I mentioned before, get more importance for recent years.

To answer this question, in this study, I tried an alternative method to predict the wind patterns with the help of RegCM4 [2] and WOCSS. WOCSS wind analysis program was developed by Ludwig et al. [3] and I used WOCSS to determine wind direction and wind speed over Canakkale Biga region for the time periods of 1970-2000, 2010-2040, 2040-2070 and 2070-2100.

As shown in Figure 1.1, I chose Canakkale Biga region in this study, because this region is the most windy region in Turkey [4]. In this research, I compared the results of given time periods in order to see how the wind direction and wind speed may change in the future. In this study, applications of the WOCSS model in Canakkale Biga region are described. Rather than the observed data from meteorological units of Canakkale Biga region, RegCM4 past and future data were obtained and used for this study. The simulated data used in this study because this study aims to show the change in the patterns of the wind at the future at

Table 1.1: Wind Energy Worldwide Top 15 countries by total wind installations, November 2015 [1].

Position 2015	**Country / Region**	**Total Capacity end of 2015 (MW)**
1	China	148.000
2	United States	74.347
3	Germany	45.192
4	India	24.759
5	Spain	22.987
6	United Kingdom	13.614
7	Canada	11.205
8	France	10.293
9	Italy	8.958
10	Brazil	8.715
11	Sweden	6.025
12	Poland	5.100
13	Portugal	5.079
14	Denmark	5.064
15	Turkey	4.718

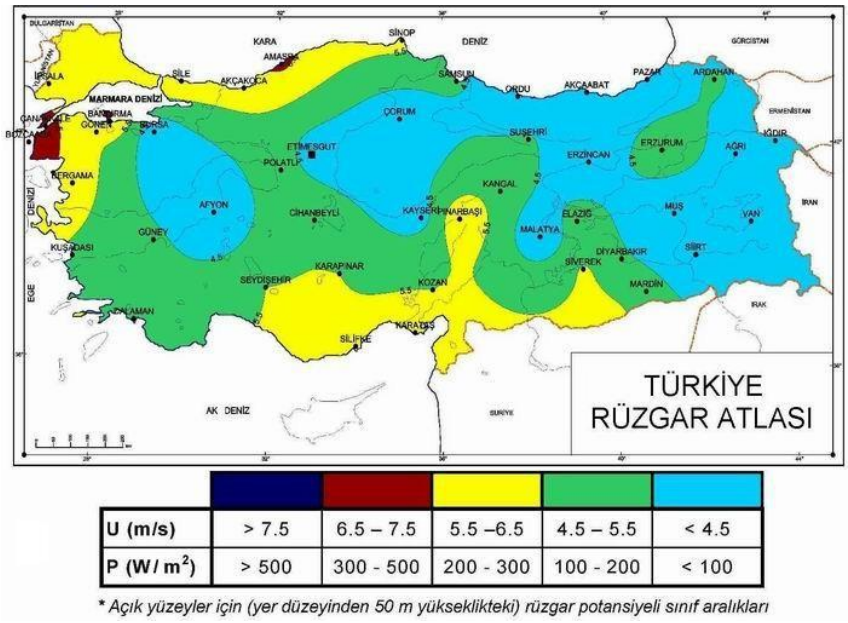

Figure 1.1: Wind Map of Turkey.

Canakkale Biga region. Specifically, for more precise results, 10 km resolution data of RegCM4 output is used. This research reveals the average of the simulated data for the periods of 1970-2000, 2010-2040, 2040-2070 and 2070-2100 from RegCM4. After obtaining data from RegCM4, WOCCS is used for the wind speed and direction predictions for Canakkale Biga region. In this process, Climate Data Operators (CDO) is used to prepare the data, and Grid Analysis and Display System (GrADS) is used to obtain the data from RegCM4 output files, and Matlab is used to create necessary WOCSS files before the WOCSS run, and also Matlab is used to create netcdf files after the WOCSS run. Netcdf files created because GrADS is compatible with netcdf files. After creating netcdf files, GrADS is used to visualize the netcdf outputs.

Moreover, wind analysis method WOCSS was firstly published by Ludwig et al. [3], and then WOCSS was used with meteorological data by Bridger et al. [5]. In order to detailed explanation of WOCSS, a manual prepared by F. L. Ludwig

at 1995 [6] and a new study was published by F. L. Ludwig and Douglas Sinton [7]. At 2006, WOCSS was compared to Coupled Ocean/Atmosphere Mesoscale Prediction System (COAMPS) model over the central California coastal region [8]. Furthermore, WOCSS was used by Vesecky et al. [9] for predicting eddies.

For the power generation analysis of the wind energy power plants of Canakkale Biga region, Karaman et al. [10] suggested that new installation of wind power plants reduce the energy import of Turkey.

This study indicates wind direction and wind speed results for given time periods for 10 meters and 50 meters outputs from WOCSS.

2. METHODOLOGY

In this section, briefly information is given about climate change, effects of climate change, and observed changes in the climate system ,IPCC, RCP Scenarios of IPCC, RegCM4 and WOCSS. After these information, the topic of how to obtain wind direction and speed results using RegCM4, GrADS, CDO, MATLAB, and WOCSS according to the climate change is summarized.

2.1. Climate Change

What is climate change? There is more than one explanation of this argument, but for point of view of MET Office; "Climate change is a large-scale, long-term shift in the planet's weather patterns or average temperatures. Earth has had tropical climates and ice ages many times in its 4.5 billion years. So what's happening now?

Since the last ice age, which ended about 11,000 years ago, Earth's climate has been relatively stable at about 14 °C. However, in recent years, the average temperature has been increasing."

According to this explanation, it is clear that the Earth's average temperature is increasing and we see effects of climate change on Earth.

There are seven main sources of evidence for climate change [11]: "Higher temperatures, changing rainfall, changes in nature, sea level rises, retreating glaciers, sea ice, and ice sheets."

Scientific research shows that the climate - that is, the average temperature of the planet's surface - has risen by 0.89 °C from 1901 to 2012. Compared with climate change patterns throughout Earth's history, the rate of temperature rise since the Industrial Revolution is extremely high.

There have been observed changes in precipitation, but not all areas have data over long periods. Rainfall has increased in the mid-latitudes of the northern hemisphere since the beginning of the 20th century. There are also changes between seasons in different regions. For example, the UK's summer rainfall is decreasing on average, while winter rainfall is increasing. There is also evidence that heavy rainfall events have become more intensive, especially over North America.

Changes in the seasons (such as the UK spring starting earlier, autumn starting later) are bringing changes in the behaviour of species, for example, butterflies appearing earlier in the year and birds shifting their migration patterns.

Since 1900, sea levels have risen by about 10 cm around the UK and about 19 cm globally, on average. The rate of sea-level rise has increased in recent decades.

Glaciers all over the world - in the Alps, Rockies, Andes, Himalayas, Africa and Alaska - are melting and the rate of shrinkage has increased in recent decades.

Arctic sea-ice has been declining since the late 1970s, reducing by about 4%, or 0.6 million square kilometres (an area about the size of Madagascar) per decade. At the same time Antarctic sea-ice has increased, but at a slower rate of about 1.5% per decade.

The Greenland and Antarctic ice sheets, which between them store the majority of the world's fresh water, are both shrinking at an accelerating rate.

2.1.1. What is causing Earth's Climate Change?

Other perspective of climate change, according to the NASA, climate change is a change in the usual weather found in a place. This could be a change in how much rain a place usually gets in a year. Or it could be a change in a place's usual temperature for a month or season.

Climate change is also a change in Earth's climate. This could be a change in Earth's usual temperature. Or it could be a change in where rain and snow usually fall on Earth.

Many things can cause climate to change all on its own. Earth's distance from the sun can change. The sun can send out more or less energy. Oceans can change. When a volcano erupts, it can change our climate.

Most scientists say that humans can change climate too. People drive cars. People heat and cool their houses. People cook food. All those things take energy. One way we get energy is by burning coal, oil and gas. Burning these things puts gases into the air. The gases cause the air to heat up. This can change the climate of a place. It also can change Earth's climate [12].

2.1.2. Observed changes in the climate system

Warming of the climate system is unequivocal, and since the 1950s, many of the observed changes are unprecedented over decades to millennia. The atmosphere and ocean have warmed, the amounts of snow and ice have diminished, and sea level has risen.

Each of the last three decades has been successively warmer at the Earth's surface than any preceding decade since 1850. The period from 1983 to 2012 was likely the warmest 30-year period of the last 1400 years in the Northern Hemisphere, where such assessment is possible (medium confidence). The globally averaged combined land and ocean surface temperature data as calculated by a linear trend show a warming of 0.85 [0.65 to 1.06] °C 2 over the period 1880 to 2012, when multiple independently produced datasets exist (Figure 2.1).

In addition to robust multi-decadal warming, the globally averaged surface temperature exhibits substantial decadal and interannual variability (Figure 2.1).

Due to this natural variability, trends based on short records are very sensitive to the beginning and end dates and do not in general reflect long-term climate trends. As one example, the rate of warming over the past 15 years (1998–2012; 0.05 [–0.05 to 0.15] °C per decade), which begins with a strong El Niño, is smaller than the rate calculated since 1951 (1951–2012; 0.12 [0.08 to 0.14] °C per decade) [13].

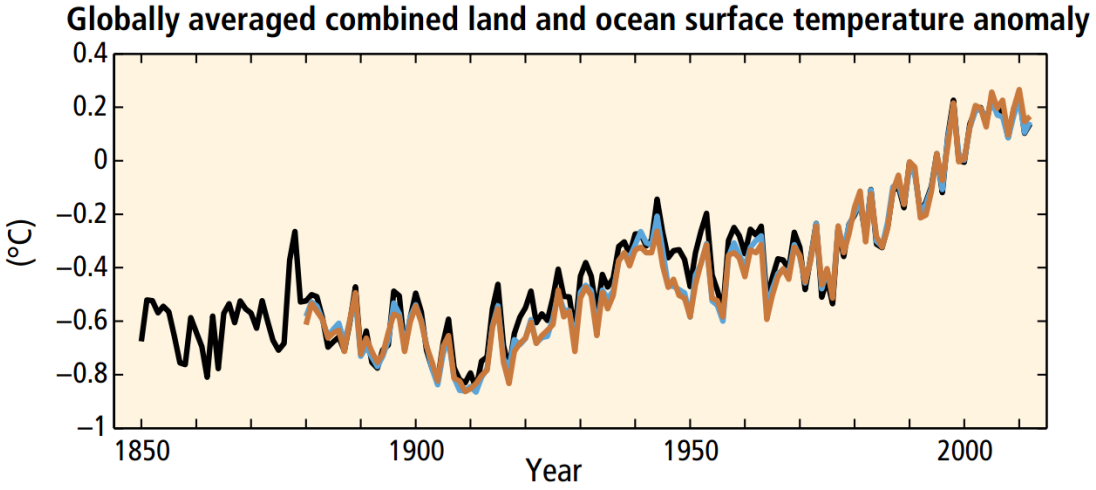

Figure 2.1: Annually and globally averaged combined land and ocean surface temperature anomalies relative to the average over the period 1986 to 2005. (Colours indicate different data sets).

2.2. IPCC

The Intergovernmental Panel on Climate Change (IPCC) is the leading international body for the assessment of climate change. It was established by the United Nations Environment Programme (UNEP) and the World Meteorological Organization (WMO) in 1988 to provide the world with a clear scientific view on the current state of knowledge in climate change and its potential environmental and socio-economic impacts. In the same year, the UN General Assembly endorsed the action by WMO and UNEP in jointly establishing the IPCC.

The IPCC reviews and assesses the most recent scientific, technical and socio-economic information produced worldwide relevant to the understanding of climate change. It does not conduct any research nor does it monitor climate related data or parameters.

2.2.1. RCP Scenarios

Representative Concentration Pathways (RCPs) are four greenhouse gas concentration trajectories adopted by the IPCC for its Fifth Assessment Report (AR5) in 2014. It supersedes Special Report on Emissions Scenarios (SRES) projections published in 2000.

The pathways are used for climate modeling and research. They describe four possible climate futures, all of which are considered possible depending on how much greenhouse gases are emitted in the years to come. The four RCPs, RCP2.6, RCP4.5, RCP6, and RCP8.5, are named after a possible range of radiative forcing values in the year 2100 relative to pre-industrial values (+2.6, +4.5, +6.0, and +8.5 W/m^2, respectively) [14]. Additionally, RCP scenarios debated in detail by van Vuuren et al. [15].

Table 2.1: Overview of RCP Scenarios

Scenario	**Description**	**Citation**
RCP 8.5	Rising radiative forcing pathway leading to 8.5 W/m^2 in 2100	Riahi et al. (2007) [16] Rao and Riahi (2006) [17]
RCP 6	Stabilization without overshoot pathway to 6 W/m^2 at stabilization after 2100	Fujino et al. (2006) [18] Hijioka et al. (2008) [19]
RCP 4.5	Stabilization without overshoot pathway to 4.5 W/m^2 at stabilization after 2100	Smith and Wigley (2006) [20] Clarke et al. (2007) [21] Wise et al. (2009) [22]
RCP 2.6	Peak in radiative forcing at 3 W/m^2 before 2100 and decline	van Vuuren et al. (2006; 2007) [23], [24]

At Table 2.1, we can see the overview of the RCP Scenarios and related publications.

Nowadays, CO_2 concentration at the atmosphere is over 400 ppm, so in this study, RCP 8.5 scenario was used for the reliability of the future predictions which tell us CO_2 concentration at the atmosphere will exceed maximum predicted concentration level before 2100 [25] .

2.3. RegCM4

I used one of regional climate model (RCM), which is RegCM4. However, RCMs needed data from general circulation models (GCM). General circulation model is a mathematical model of the circulation of the Earth's atmosphere and ocean. Atmospheric and oceanic GCMs are key components of global climate models along with sea ice and land-surface components. GCMs and global climate models are widely applied for weather forecasting, understanding the climate, and projecting climate change [26]. Regional climate model is a numerical climate prediction model forced by specified lateral and ocean conditions from a general circulation model (GCM) or observation-based dataset (reanalysis) that simulates atmospheric and land surface processes, while accounting for high-resolution topographical data, land-sea contrasts, surface characteristics, and other components of the Earth-system [27].

The Regional Climate Model system RegCM , originally developed at the National Center for Atmospheric Research (NCAR), is maintained in the Earth System Physics (ESP) section of the ICTP. The first version of the model, RegCM1, was developed in 1989 and since then it has undergone major updates in 1993 (RegCM2), 1999 (RegCM2.5), 2006 (RegCM3) and most recently 2010 (RegCM4). The latest version of the model, RegCM4, is now fully supported by the ESP, while previous versions are no longer available. This version includes major upgrades in

the structure of the code and its pre- and post- processors, along with the inclusion of some new physics parameterizations. The model is flexible, portable and easy to use. It can be applied to any region of the world, with grid spacing of up to about 10 km (hydrostatic limit), and for a wide range of studies, from process studies to paleoclimate and future climate simulation [28]. At this hydrostatic limit, model assumes that air parcel moves only horizontal and vertical, not diagonally.

2.3.1. Model Components

The RegCM modeling system has four components: Terrain, ICBC, RegCM, and Postprocessor. Terrain and ICBC are the two components of RegCM preprocessor. Terrestrial variables (including elevation, landuse and sea surface temperature) and three-dimensional isobaric meteorological data are horizontally interpolated from a latitude longitude mesh to a high-resolution domain on either a Rotated (and Normal) Mercator, Lambert Conformal, or Polar Stereographic projection. Vertical interpolation from pressure levels to the σ coordinate system of RegCM is also performed. σ surfaces near the ground closely follow the terrain, and the higher-level σ surfaces tend to approximate isobaric surfaces.

Since the vertical and horizontal resolution and domain size can vary, the modeling package programs employ parameterized dimensions requiring a variable amount of core memory, and the requisite hard-disk storage amount is varied accordingly.

2.3.2. The RegCM Model Horizontal and Vertical Grid

It is useful to first introduce the model's grid configuration. The modeling system usually gets and analyzes its data on pressure surfaces, but these have to be interpolated to the model's vertical coordinate before input to the model. The vertical coordinate is terrain-following (Figure 2.6) meaning that the lower

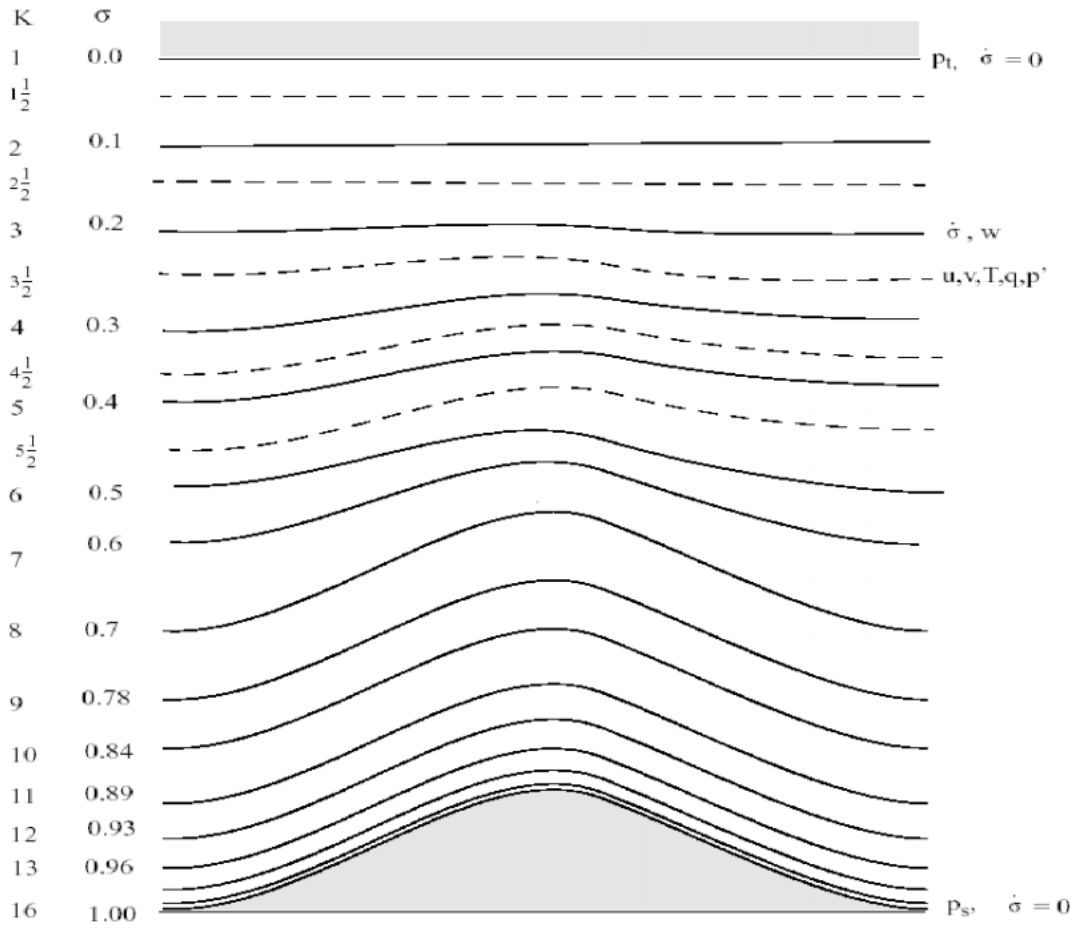

Figure 2.2: Schematic representation of the vertical structure of the model. This example is for 16 vertical layers. Dashed lines denote half-sigma levels, solid lines denote full-sigma levels. (Adapted from the PSU/NCAR Mesoscale Modeling System Tutorial Class Notes and User's Guide.

grid levels follow the terrain while the upper surface is flatter. Intermediate levels progressively flatten as the pressure decreases toward the top of the model.

The Hydrostatic solver uses A dimensionless σ coordinate to define the model levels where p is the pressure, p_t is a specified constant top pressure, p_s is the surface pressure.

$$\sigma = \frac{p - p_t}{p_s - p_t} \tag{2.1}$$

where we can define:

$$p^*(x, y) = p_s(x, y) - p_t \tag{2.2}$$

For the Non-hydrostatic solver a similar dimensionless coordinate is used, but it is defined entirely from the reference pressure. Given a reference atmospheric profile:

$$p(x, y, z, t) = p_0(z) - p'(x, y, z, t) \tag{2.3}$$

$$T(x, y, z, t) = T_0(z) - T'(x, y, z, t) \tag{2.4}$$

$$\rho(x, y, z, t) = \rho_0(z) - \rho'(x, y, z, t) \tag{2.5}$$

the vertical sigma coordinate is defined as:

$$\sigma = \frac{p_0 - p_t}{p_s - p_t} \tag{2.6}$$

where p_s is the surface pressure, p_t is a specified constant top pressure and p_0 is the reference pressure profile. The total pressure at each grid point is thus given as:

$$p = p^{*}\sigma + p_t + p' \tag{2.7}$$

with p^* defined as in the hydrostatic solver.

It can be seen from the equation and Figure 2.6 that σ is zero at the top and one at the surface, and each model level is defined by a value of σ. The model vertical resolution is defined by a list of values between zero and one that do not necessarily have to be evenly spaced. Commonly the resolution in the boundary layer is much finer than above, and the number of levels may vary upon the user demand.

The horizontal grid has an Arakawa-Lamb B-staggering of the velocity variables with respect to the scalar variables. This is shown in Figure 2.7 where it can be seen that the scalars (T, q, p, etc) are defined at the center of the grid box, while the eastward (u) and northward (v) velocity components are collocated at the corners. The center points of grid squares will be referred to as cross points, and the corner points are dot points. Hence horizontal velocity is defined at dot points. Data is input to the model, the preprocessors do the necessary interpolation to assure consistency with the grid.

All the above variables are defined in the middle of each model vertical layer, referred to as half-levels and represented by the dashed lines in Figure 2.6. Vertical velocity is carried at the full levels (solid lines). In defining the sigma levels it is the full levels that are listed, including levels at $\sigma = 0$ and 1. The number of model layers is therefore always one less than the number of full sigma levels.

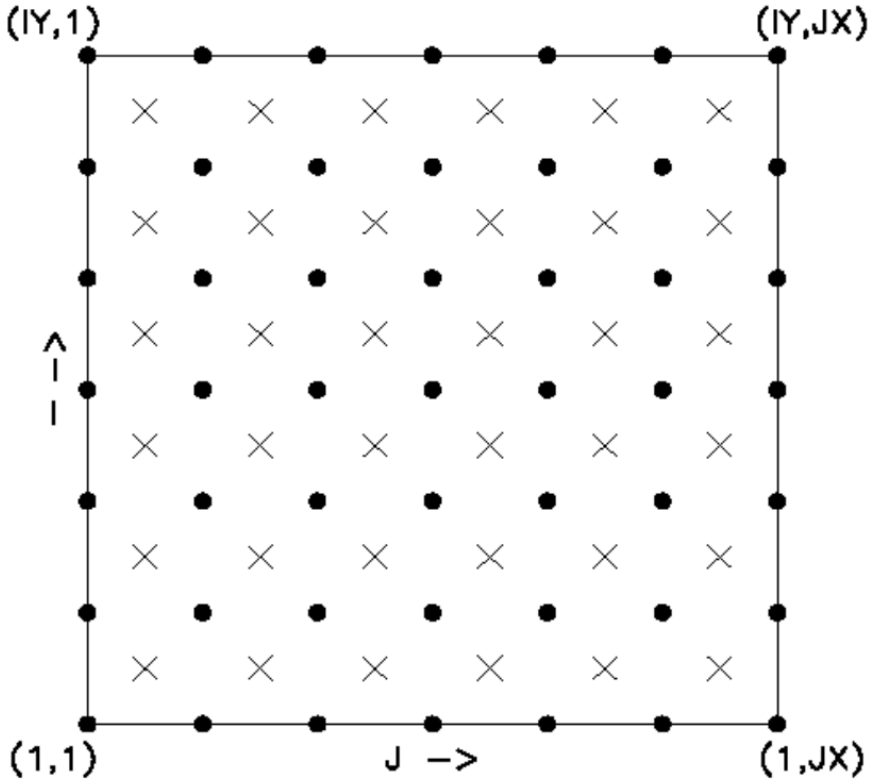

Figure 2.3: Schematic representation showing the horizontal Arakawa B-grid staggering of the dot and cross grid points.

The finite differencing in the model is, of course, crucially dependent upon the grid staggering wherever gradients or averaging are represented terms in the equation.

Detailed information given in the Reference Manual of RegCM4.5 by ICTP [29].

2.3.3. ERA-Interim Dataset

This dataset is produced by European Centre for Medium-Range Weather Forecasts. ERA-Interim is a global atmospheric reanalysis from 1979, continuously updated in real time. [30] .

2.4. WOCSS

Detailed description of WOCSS explained by F. L. Ludwig and Douglas Sinton [7]. Very briefly, the model uses critical streamline concepts to define flow surfaces, from observed winds and temperature profile(s), that may intercept higher terrain features when the atmosphere has a stable stratification. Then when the flow on these surfaces is iteratively adjusted toward two-dimensional non diveregence of the fluxes between surfaces, the flow is forced around orographic obstructions [6].

WOCSS is based on Fortran and before the WOCSS run, WOCSS needs some files, which are WOCSS.f, rundat.dat, terrain.dat, winds.dat. These files were explained more detailed in the A Guide To The Winds On Critical Streamline Surfaces (WOCSS) Code, Salt Lake City Area Data And Other Related Files from F. L. Ludwig [6].

2.4.1. Methodology of WOCSS

WOCSS treats the problem in a three dimensional domain having the directions x, y and σ. By defining σ direction, it becomes easier to define terrain following surfaces that lie almost parallel both to the original terrain and to each other.

WOCSS first uses the inverse distance weighing method in order to extrapolate the input wind data and to form the first flow surface that contains surface wind information and estimates the remaining flow surfaces, afterwards. Flow surfaces are not defined with respect to a certain intermediate distance, but they are defined in terms of a physical phenomenon, which is called critical dividing streamline principle [31].

Critical dividing streamline principle assumes that the work done by an air parcel against the buoyant restoring force is equal to the original kinetic energy of that air parcel. With this assumption one can determine the maximum height that each air parcel can rise by using the following formula, Equation (2.8), (Sheppard's formula), where T , is defined as the average temperature between Z_{max} and Z_0 [7]

$$Z_{\max} - Z_0 = V_0(\frac{\delta\theta}{\delta z}\frac{g}{T})^{-1/2} \tag{2.8}$$

According to Equation (2.8) the height that each air parcel can reach is determined. By combining those calculated heights with the topographic profile, rest of the flow surfaces throughout the atmosphere is calculated. Formations of the flow surfaces, make the atmosphere stratified and it is assumed that there is no flow between those flow surfaces, i.e. the velocity in σ direction is zero. That final assumption eliminates one parameter from the problem. In other words, by using this principle, the 3D problem is divided into several 2D problems, which makes the main problem easier to solve. These coordinate surfaces will not only approximate the shape of

the flow, but they will also intersect the terrain in areas where the flow cannot pass over it [3].

After all the flow surfaces are formed, following goal is to make the flow surfaces compatible with the terrains. The WOCSS model imposes mass conservation as a non-divergence constraint to force the flow interact with the terrain. If any flow surface intersects with a terrain surface, the wind speed under that intersection point is set to be equal to zero. That ensures, there is no wind within the landforms, which is a very fundamental physical requirement for a plausible solution.

Lastly, the flow is adjusted so that the divergence is approximately, but not exactly, equal to zero. The iterative scheme described by Endlich [31] is used to adjust the wind estimations on flow surfaces to satisfy Equation (2.9), where the flux variables are formulated as in Equation (2.10) and Equation (2.11). Satisfying those formulations, WOCSS model iteratively adjusts the flow on each surface toward two-dimensional (within the critical streamline surfaces) non-divergence. That last adjustment forces the wind to flow around the terrains, so that model outputs more realistic solutions also around the terrains [3].

$$\frac{\delta u'}{\delta x} + \frac{\delta v'}{\delta y} = 0 \tag{2.9}$$

$$u' = u\Delta z \tag{2.10}$$

$$v' = v\Delta z \tag{2.11}$$

2.4.2. Input Files of WOCSS

WOCSS needs three different input files which are rundat.dat (see Figure C.1), terrain.dat and winds.dat (see Figure C.2). rundat.dat file contains:

(i) Nskip ASCII option that writes every nskip grid points in x & y,

(ii) Number of flow surfaces used for calculations,

(iii) σ values of those flow levels separated with comma beginning from 0 and ending with 1,

(iv) Number of flat surfaces, depending on which output flow surfaces will be determined,

(v) Heights of those flow surfaces separated with a comma (Either in meters or in feet. One should change the conversion factor accordingly),

(vi) Number of wind sites (It should be chosen greater than the actual number of wind sites, i.g.200), number of upper wind station and number of radiosonde,

(vii) Speed conversion factor to adjust the speeds if they are not in meters per second (Given speed data will be multiplied by this conversion factor within the program. Conversion factor should be 1.0 if the speed data are in meters per second.), height conversion factor to adjust the heights if they are not in meters (Given height data will be multiplied by this conversion factor within the program. Conversion factor should be 1.0 if the height data are in meters.),

(viii) Number of rows and number of columns of the working domain (Maximum value for the number of rows is 123 and maximum value for the number of columns is 108),

(ix) Grid spacing in kilometers,

(x) UTMX and UTMY coordinates of the reference point that will be used for the calculations,

(xi) x and y indices of the chosen reference point (When the indices are chosen to be 1,1, the reference point is actually the southwest corner of the studied region. One should pay attention to that point, otherwise the outputs would

be totally cumbersome),

(xii) Height of the top surface over low point in meters,

(xiii) Slope factor that will be used for the first guess wind estimations (0=flat,1=terrain following),

(xiv) Minimum theta lapse rate that will be used for flow surface estimations throughout the atmosphere (The smaller the number, the less will be the rise.),

(xv) Surface roughness length in meters (That is close to zero, but not exactly zero) and anemometer height in meters,

(xvi) Minimum distance for interpolation weighing (0.1 enables reasonable outputs in general),

(xvii) Distance weighing power (2.0 enables reasonable outputs in general), Distance weighing power (2.0 enables reasonable outputs in general),

(xviii) Iteration limit in subroutine bal5 (20 enables reasonable outputs in general),

(xix) Maximum adjustment factor near observation sites (0=No adjustments, 0.2 enables reasonable outputs in general),

(xx) Indices of first low point around the radiosonde,

(xxi) Indices of second low point around the radiosonde,

(xxii) Indices of third low point around the radiosonde,

(xxiii) Indices of fourth low point around the radiosonde,

(xxiv) Indices of fifth low point around the radiosonde,

(xxv) Number of cases before stopping.

For the second input file of WOCSS, winds.dat file contains:

(i) Hour, month, day, year (This data does not have any effect on the calculations and only read by the program as they are written in their order),

(ii) idop values that will be read in the subroutine geosig and be used later on (Five integers should be given without any comma between them),

(iii) itmp values that will be read in the subroutine geosig and be used later on (Five integers should be given without any comma between them),

(iv) Number of surface observation sites (At least one surface observation site should be present),

(v) Following data of the i th surface observation site should be given in order: UTMX coordinate in kilometers, UTMY coordinate in kilometers, pressure in milibars (mb), temperature in degrees Celcius (°C), wind direction in degrees, wind speed (There is not any certain unit for wind speed format, but it is only of importance that all the surface observation site wind speeds have the same unit and the necessary speed conversion factor is given in the rundat.dat file.); for (i-1) more times, the above data should be given in a separate line; one line for each individual surface observations. The order, in which the surface observation sites are given are not of importance. The program will read the data and find the surface observation site locations individually.),

(vi) UTMX and UTMY coordinates of the upper wind station in kilometers,

(vii) Number of levels throughout atmosphere, that the upper wind station data have separate values for each,

(viii) Height of the j th level in meters(or in feet, height conversion factor should be given accordingly in rundat.dat file), wind direction in degrees, wind speed (Unit should be consistent with the previous wind speed units in winds.dat file); for (j-1) more times, the above data should be given in a separate line; one line for each individual level,

(ix) UTMX and UTMY coordinates of the radiosonde in kilometers,

(x) Number of levels throughout the atmosphere that the the radiosonde data have separate values for each; the number indicating the format of the following data will have,

(xi) Height of the k th level in meters(or in feet, height conversion factor should be given accordingly in rundat.dat file), wind direction in degrees, wind speed (Units should be consistent with the previous wind speed units in winds.dat file); for (k-1) more times, the above data should be given in a separate line; one line for each individual level,

(xii) The data in (vii.) and (viii.) should be re-written, because the program calls

the subroutine in which those part is read twice.

2.5. PROCESS

WOCSS used with observed meteorological data on the study of San Francisco Bay Area, Bridger et al. [5] and the study of Terrain Induced Wind Profiles by Evren Bayraktar for the wind patterns of Istanbul and the Bosporus [32]. However, in this study, rather than observed data I used simulated data from RegCM4.

To obtain 10 km resolution RegCM4 output data, firstly, I ran RegCM4, using MPI dataset, which is obtained from Max Planck Institute for Meteorology and MPI dataset is one of the GCM datasets and MPI dataset is at 150 km resolution, to increase the resolution to 50 km. Then, I used the outputs of this run as an input of second RegCM4 run, which is called nested RegCM4 run. In other words, first run of RegCM4 output data, which is 50km resolution,was used as an input for second RegCM4 run. After second RegCM4 run, I increased the resolution at 10 km. In addition, I use Reference (RF) mode of RegCM4 for the period of 1970-2000 and for the 2010-2040 and so on periods, I use the scenario based on RCP8.5 which developed and published by IPCC.

Basically, WOCSS needs two types of meteorological observation data. First one is surface weather observation data and second one is radiosonde data. Surface weather observation data contain pressure (mbar), temperature (K), wind direction and speed (m/s) values. Radiosonde data contain pressure (mbar), height (m), temperature (K), wind direction and speed (m/s) values. The difference between surface data and radiosonde data is the pressure levels. In addition to these variables, WOCSS use UTM x and y coordinates but in this study, I use Matlab script "deg2utm" (See Figure A.1) to convert from latitude and longitude coordinates to UTM coordinates.

Before using WOCSS, I prepare terrain file named “biga990.dat”. This file contains topography feature of Canakkale Biga region. This file filled with numbers which related to the topography. There are two different ways to obtain topography. One approach is to use GrADS with GMTED_DEM_30s.nc. In this way, I open the GMTED_DEM_30s.nc file in GrADS and I specify the latitude and longitude, then I print the data to csv file. After this, I convert csv file to dat file. Another approach is to use the web site earthexplorer.usgs.gov, which contains topography maps provided via NASA’s Shuttle Radar Topography Mission with the permission of NASA (See Figure A.2) [33].

After the RegCM4 run, I use ATM files which contain atmospheric variables with location, that are longitude, latitude, land mask, topography, pressure, total precipitation flux, ground temperature, westerly and southerly wind, air temperature, specific humidity, relative humidity. I use CDO to merge thirty years of RegCM4 ATM output files to one file, and use CDO to take an average of thirty years. And, I use sigma2p to convert ATM files to ATM pressure files. After that, I, again, use CDO to merge thirty years of RegCM4 ATM pressure files to one file, and use CDO to take an average of thirty years. Then I use GrADS and GrADS’ scripts to obtain needed information as csv files for WOCSS. After that, I use Linux bash scripts to organize all csv files for the Matlab use. Before using Matlab, I prepare an excel file coordinates.xlsx that contains both surface and radiosonde coordinates (See Figure B.1). Later, I write and use a Matlab code createexcel.m (see Figure A.3) to create an excel file canakkale2010-2040.xlsx (see Figure B.2) to use another Matlab code wocss.m (see Figure A.4) which creates needed WOCSS files that are rundat.dat (see Figure C.1), terrain.dat, and winds.dat (see Figure C.2). Later, I copy WOCSS fortran code file and the control.dat file to the same folder with the other dat files. Afterwards, I use ifort to execute WOCSS fortran code and then run the executable file and get the WOCSS results. Thereafter, I use Matlab to create netcdf file using data inside the windsuv.out file. Finally, I use GrADS to visualize the netcdf file.

3. RESULTS

In this section, I will show the wind direction and speed results of time periods of 1970-2000, 2010-2040, 2040-2070, and 2070-2100 at 10m and 50m heights. I chose 10m because of the geographical limits for the wind and 50m for the height of the hub of the wind energy power plants.

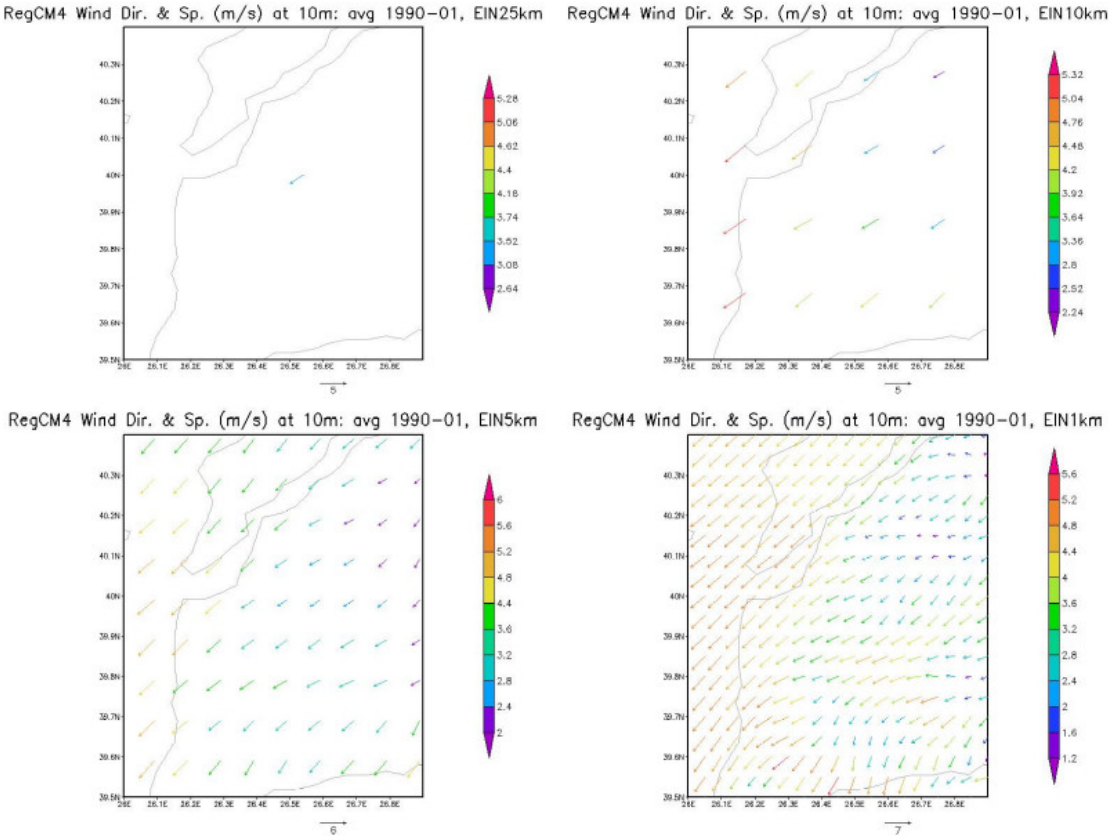

Figure 3.1: Wind direction and speed comparison of the different resolutions

Before the results, I demonstrate the importance of the 1km resolution. I and my friends study RegCM4 at maximum 10 km resolution until this May. This May, we ran RegCM4 at 25 km, 5 km and 1 km resolution at ICTP. However, this version of RegCM4 is at the beta state and RegCM4 run at 1km resolution takes much time

and needs more computer power and storage capacity than WOCSS.

As you can see in Figure 3.1, RegCM4 outputs show us the importance of the high resolution. For this moment, this figure just indicates the average of the January of 1990. Unfortunately, running RegCM4 at 1 km resolution is not available and it is costly at that moment publicly. For these reasons, WOCSS is a good alternative to increase the resolution to 1 km with following topography.

3.1. Wind Direction and Speed Results for the Period of of 1970-2000

3.1.1. Wind Speed at 10 meters

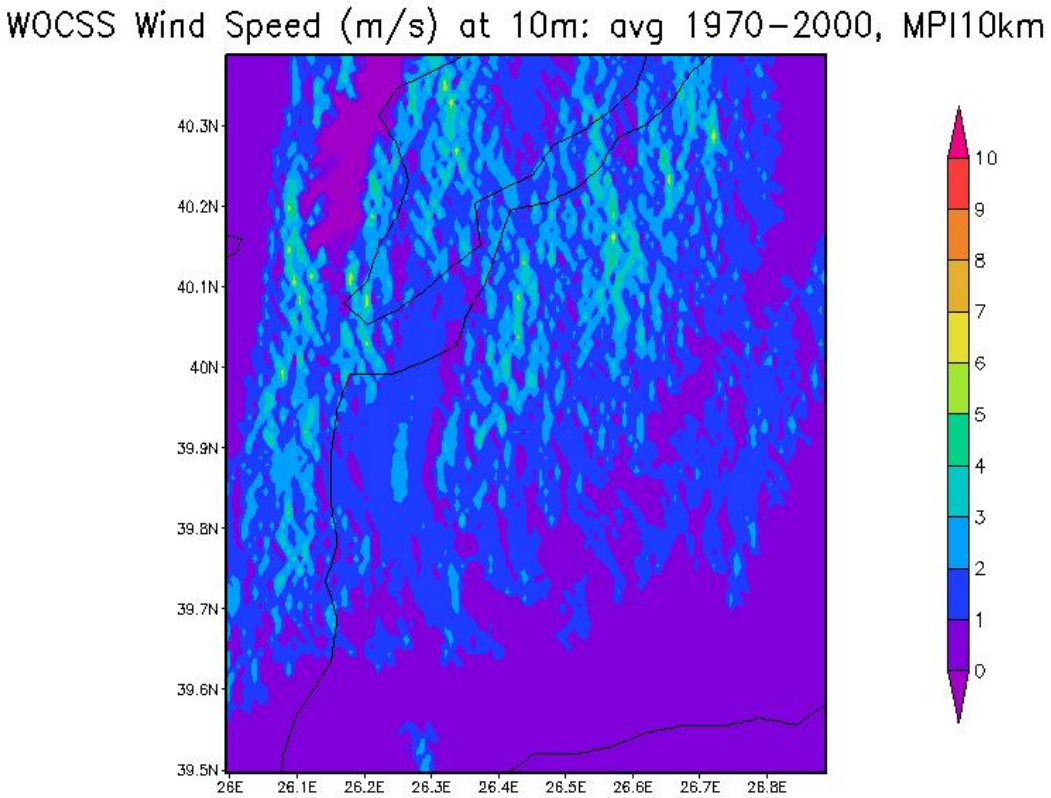

Figure 3.2: WOCSS wind speed (m/s) result at 10m: avg of 1970-2000

At Figure 3.2, for the average of the period of 1970-2000 at 10m height, maximum wind speed is 6.69 m/s.

3.1.2. Wind Direction at 10 meters

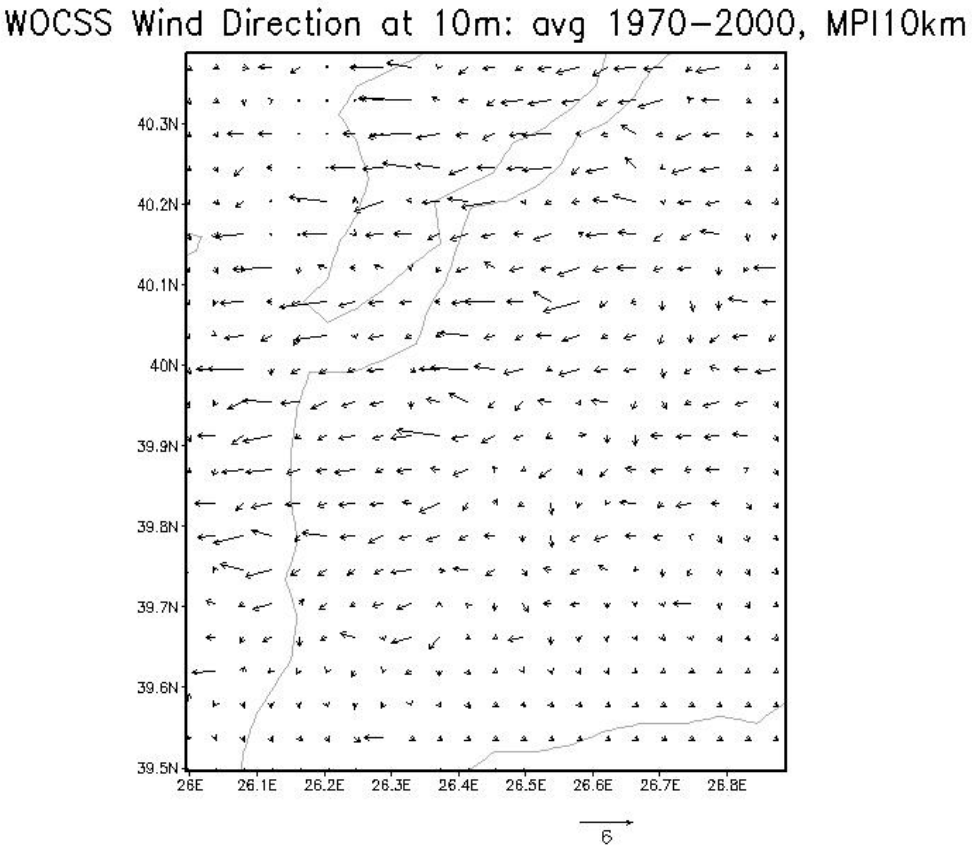

Figure 3.3: WOCSS wind direction result at 10m: avg of 1970-2000

At Figure 3.3, for the average of the period of 1970-2000 at 10m height, the high-speed wind is distributed around the bosporus and the north of the region.

3.1.3. Wind Speed at 50 meters

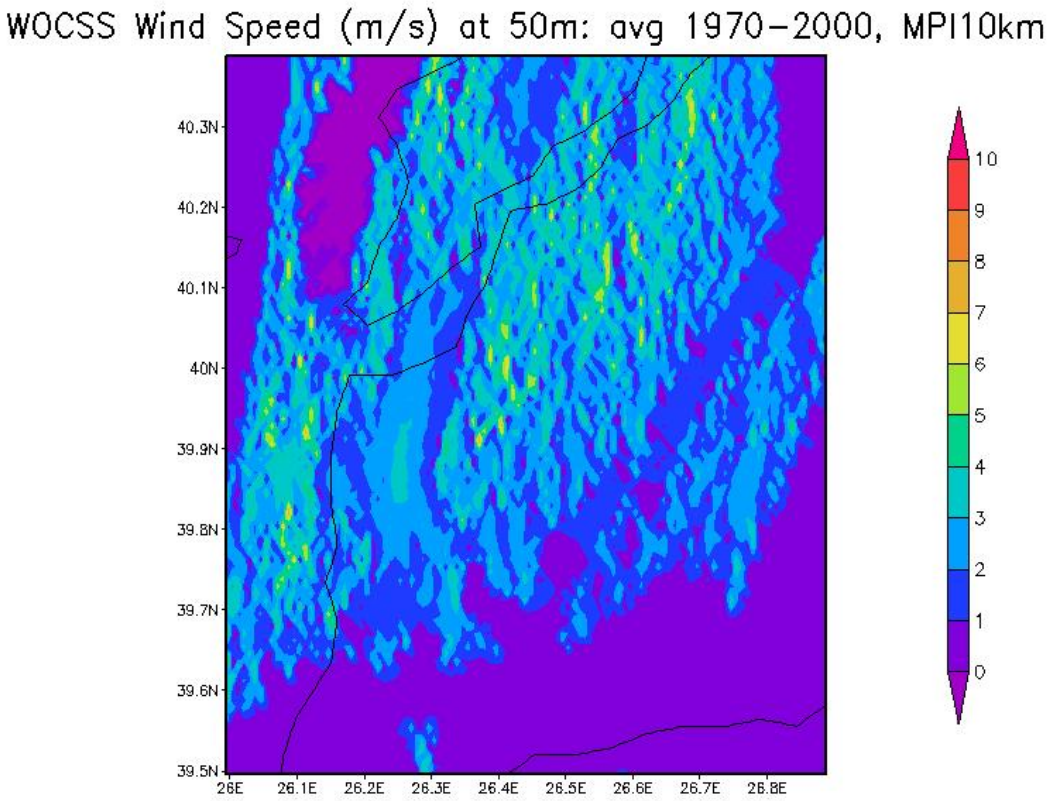

Figure 3.4: WOCSS wind speed (m/s) result at 50m: avg of 1970-2000

At Figure 3.4, for the average of the period of 1970-2000 at 50m height, maximum wind speed is 7.69 m/s and this is 1 m/s more than at 10m height at this time period.

3.1.4. Wind Direction at 50 meters

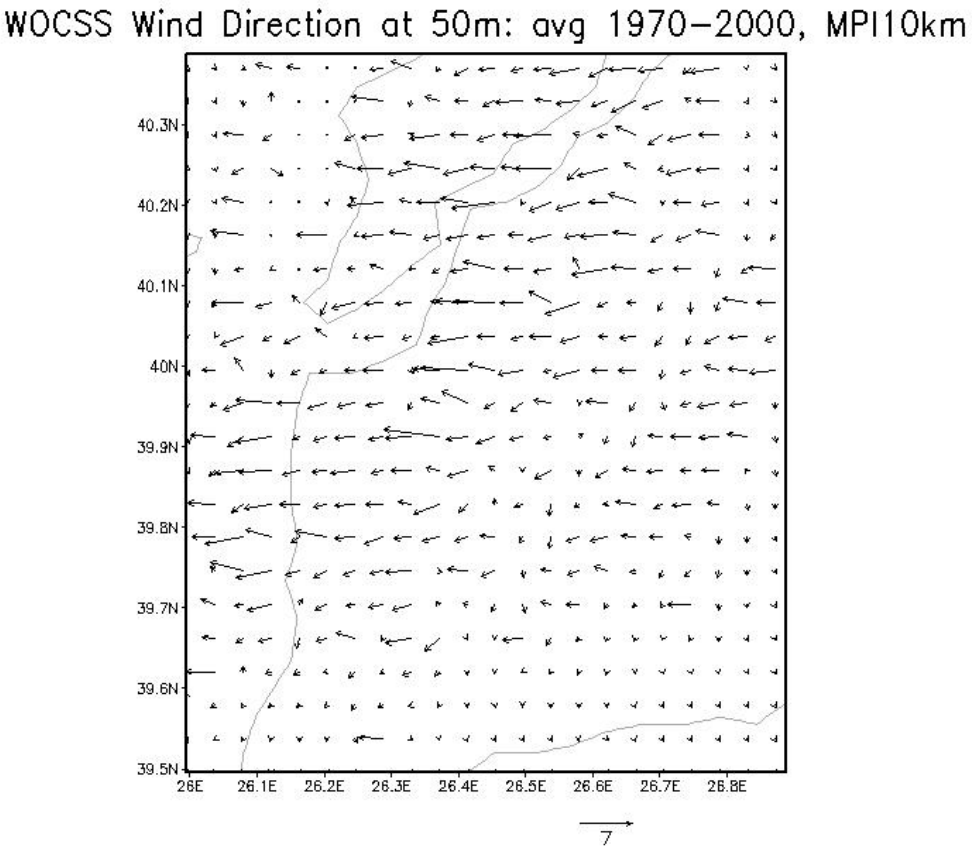

Figure 3.5: WOCSS wind direction result at 50m: avg of 1970-2000

At Figure 3.5, for the average of the period of 1970-2000 at 50m height, the high-speed wind is distributed around the bosporus and the north and northwest of the region.

3.2. Wind Direction and Speed Results for the Period of of 2010-2040

3.2.1. Wind Speed at 10 meters

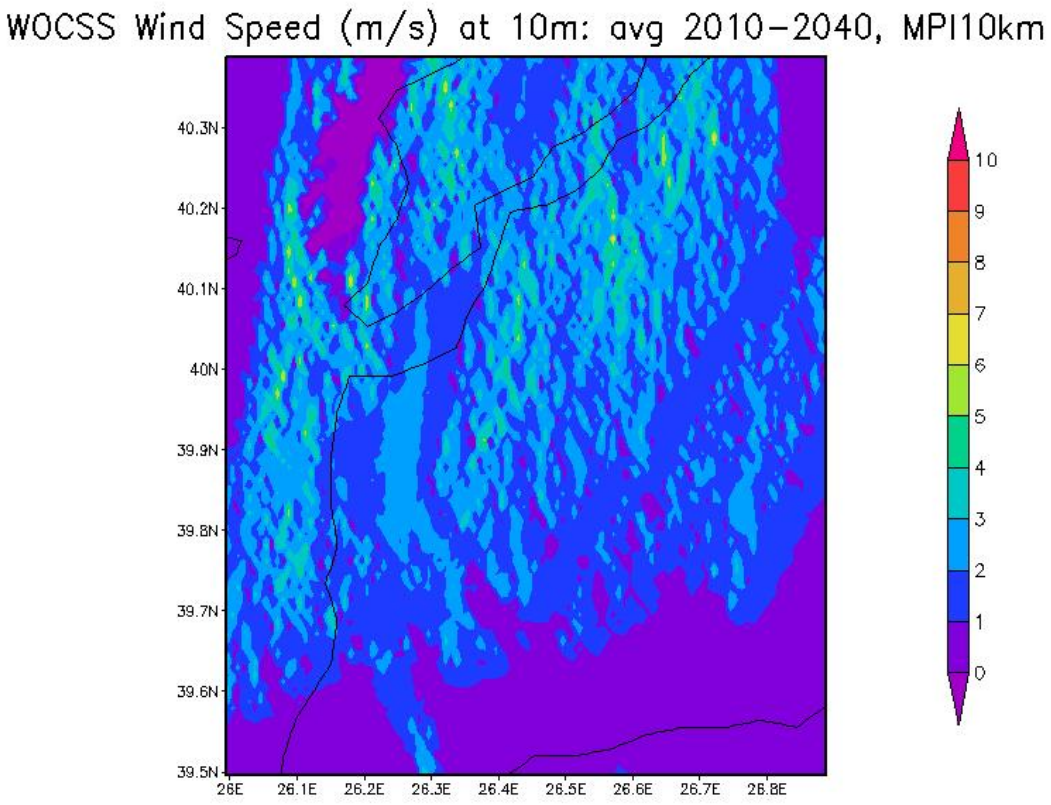

Figure 3.6: WOCSS wind speed (m/s) result at 10m: avg of 2010-2040

At Figure 3.6, for the average of the period of 2010-2040 at 10m height, maximum wind speed is 7 m/s and this is 0.31 m/s more than at 10m height at the average of the period of 1970-2000.

3.2.2. Wind Direction at 10 meters

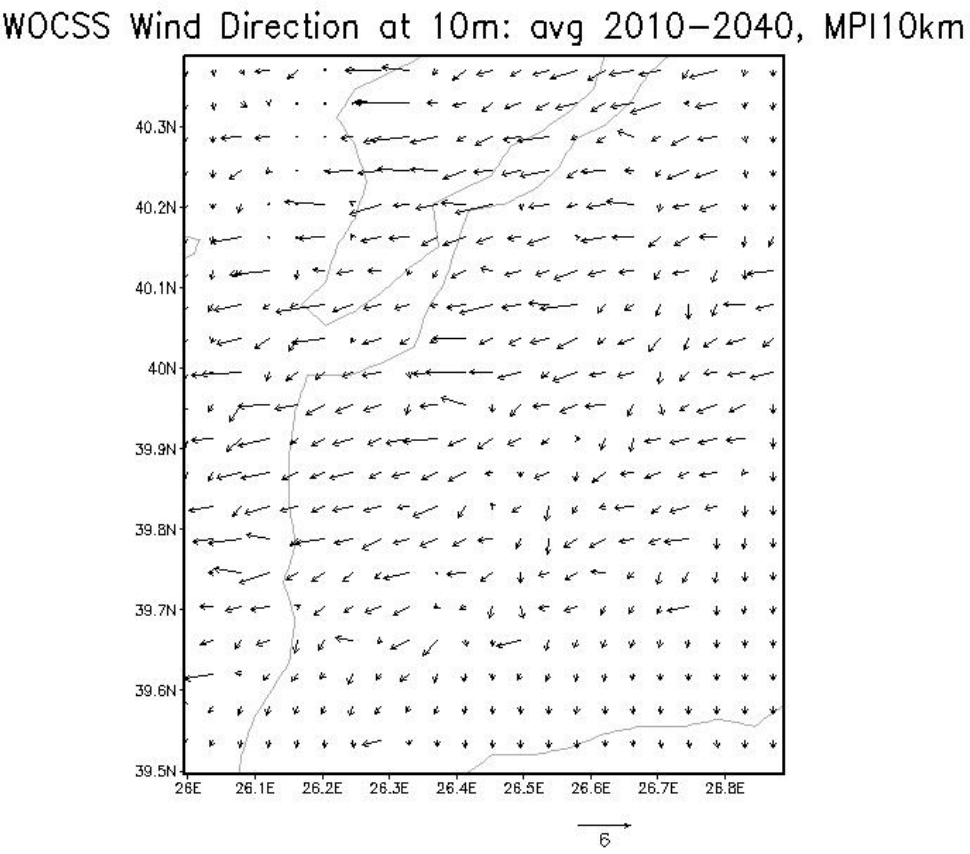

Figure 3.7: WOCSS wind direction result at 10m: avg of 2010-2040

At Figure 3.7, for the average of the period of 2010-2040 at 10m height, the high-speed wind is distributed around the bosporus and the north and northwest of the region.

3.2.3. Wind Speed at 50 meters

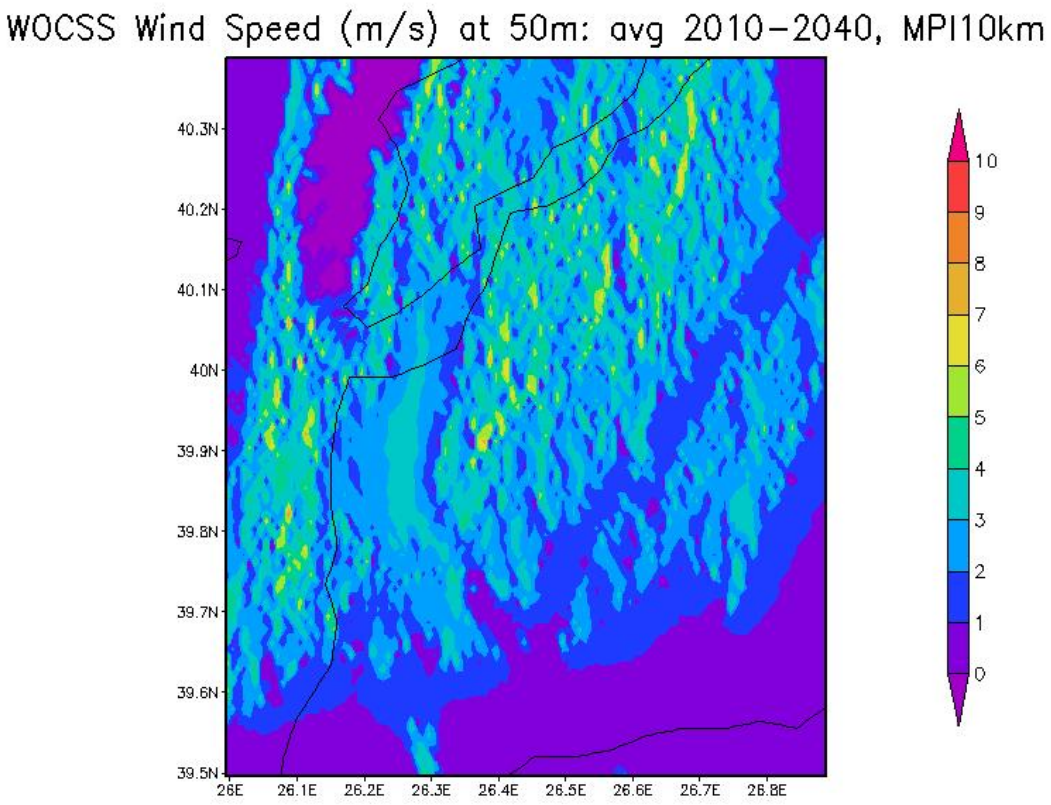

Figure 3.8: WOCSS wind speed (m/s) result at 50m: avg of 2010-2040

At Figure 3.8, for the average of the period of 2010-2040 at 50m height, maximum wind speed is about 8.08 m/s and this is 1.08 m/s more than at 10m height at this time period and this is 0.39 m/s more than the average of the period of 1970-2000 at 50m height.

3.2.4. Wind Direction at 50 meters

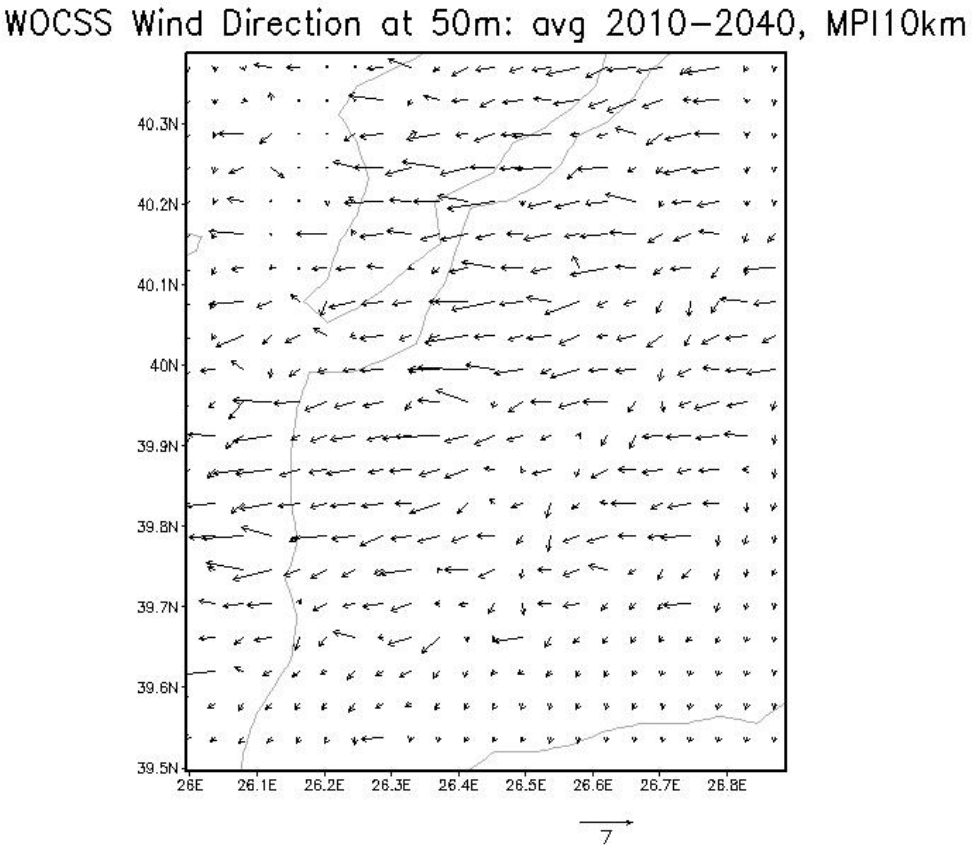

Figure 3.9: WOCSS wind direction result at 50m: avg of 2010-2040

At Figure 3.9, for the average of the period of 2010-2040 at 50m height, the high-speed wind is distributed around the bosporus and the middle and the north of the region.

3.3. Wind Direction and Speed Results for the Period of of 2040-2070

3.3.1. Wind Speed at 10 meters

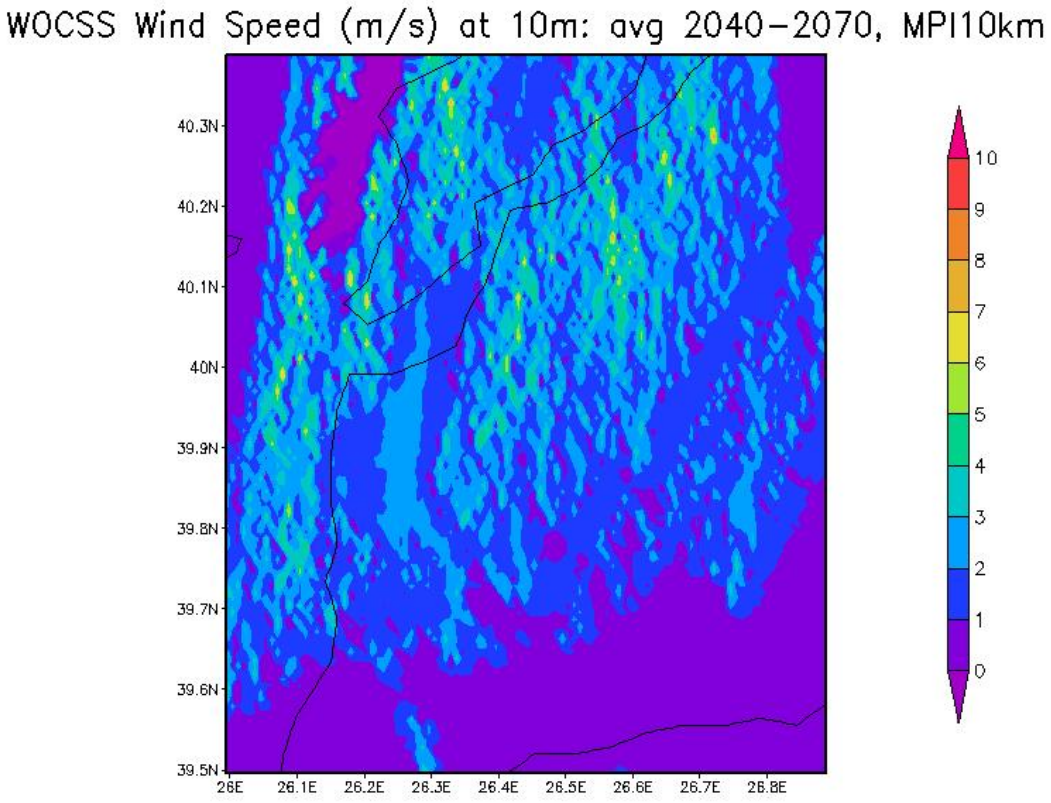

Figure 3.10: WOCSS wind speed (m/s) result at 10m: avg of 2040-2070

At Figure 3.10, for the average of the period of 2040-2070 at 10m height, maximum wind speed is about 7.85 m/s and this is 0.85 m/s more than the average of the period of 2010-2040 at 10m height.

3.3.2. Wind Direction at 10 meters

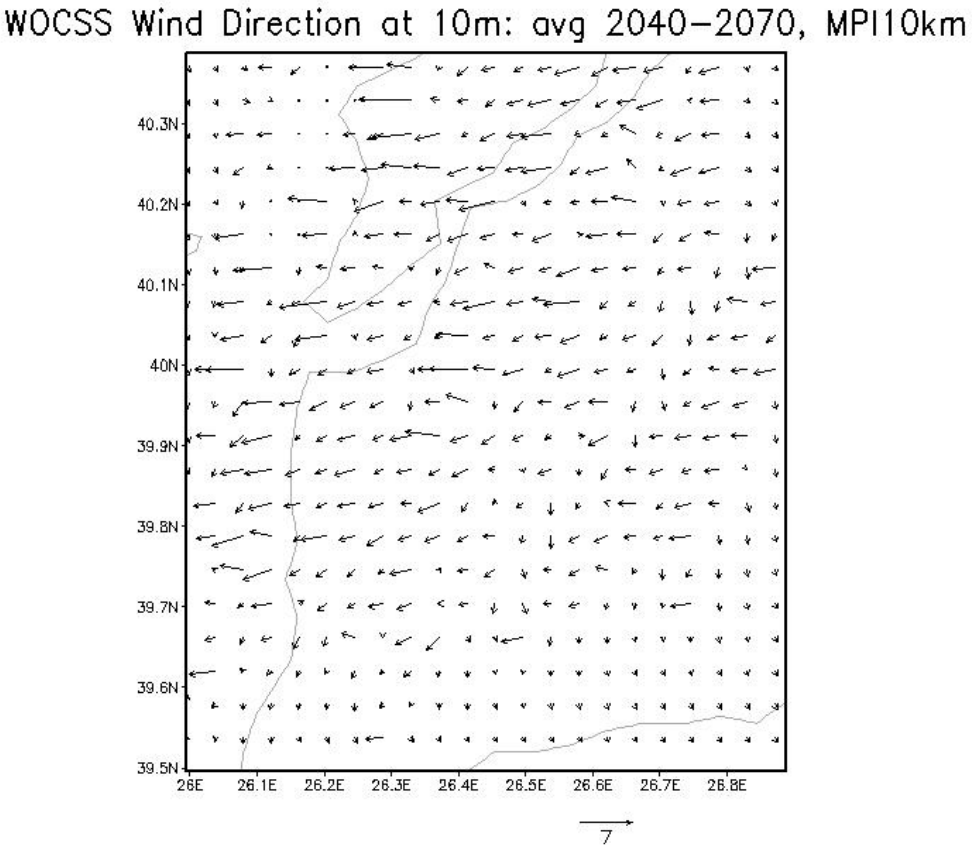

Figure 3.11: WOCSS wind direction result at 10m: avg of 2040-2070

At Figure 3.11, for the average of the period of 2040-2070 at 10m height, the high-speed wind is distributed around the bosporus.

3.3.3. Wind Speed at 50 meters

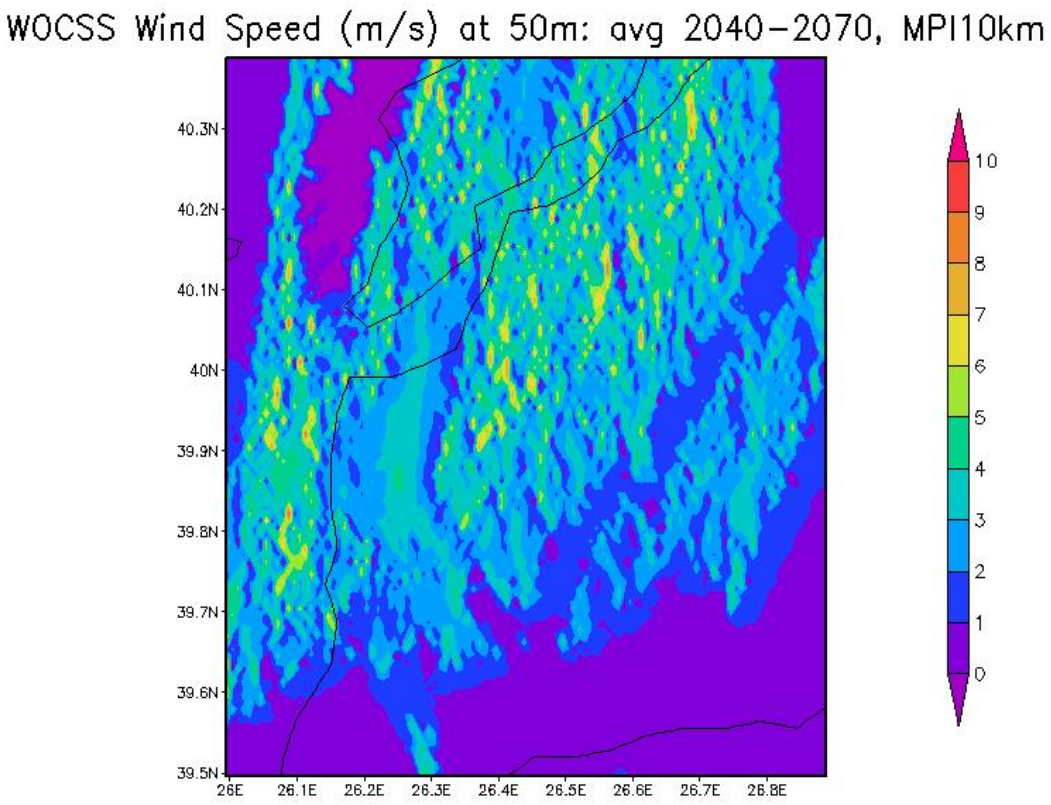

Figure 3.12: WOCSS wind speed (m/s) result at 50m: avg of 2040-2070

At Figure 3.12, for the average of the period of 2040-2070 at 50m height, maximum wind speed is about 9.0 m/s and this is 1.15 m/s more than at 10m height at this time period and this is 0.92 m/s more than the average of the period of 2010-2040 at 50m height.

3.3.4. Wind Direction at 50 meters

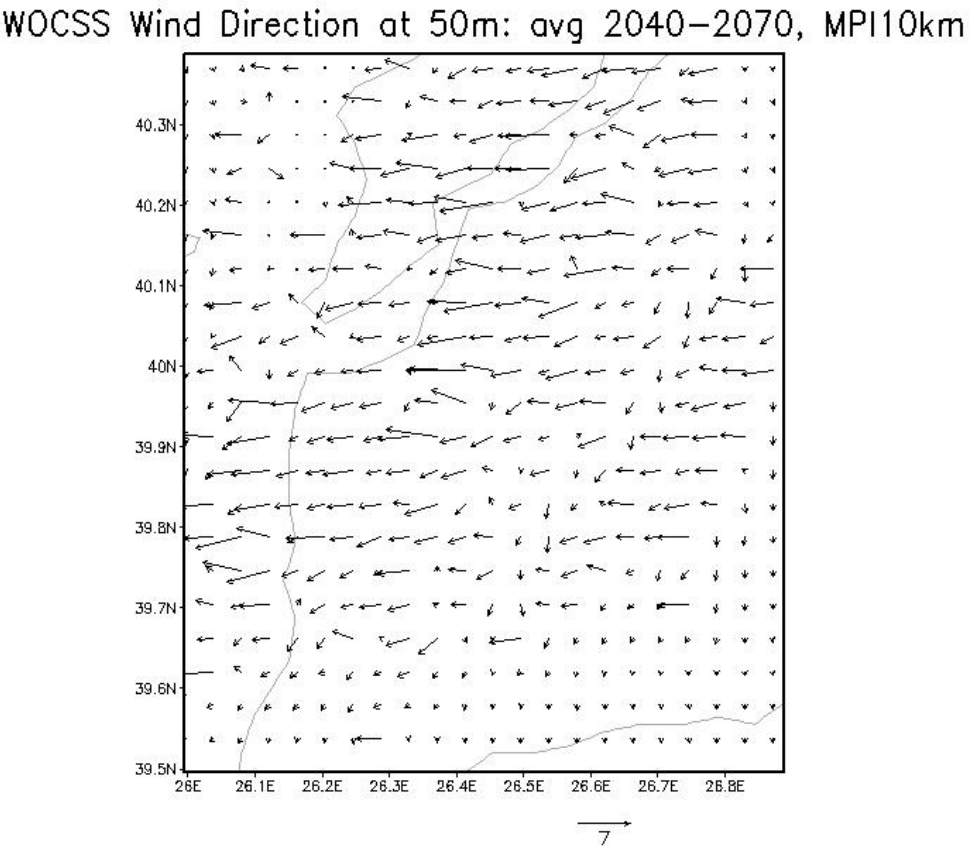

Figure 3.13: WOCSS wind direction result at 50m: avg of 2040-2070

At Figure 3.13, for the average of the period of 2040-2070 at 50m height, the high-speed wind is distributed around the bosporus and the middle and the north of the region.

3.4. Wind Direction and Speed Results for the Period of of 2070-2100

3.4.1. Wind Speed at 10 meters

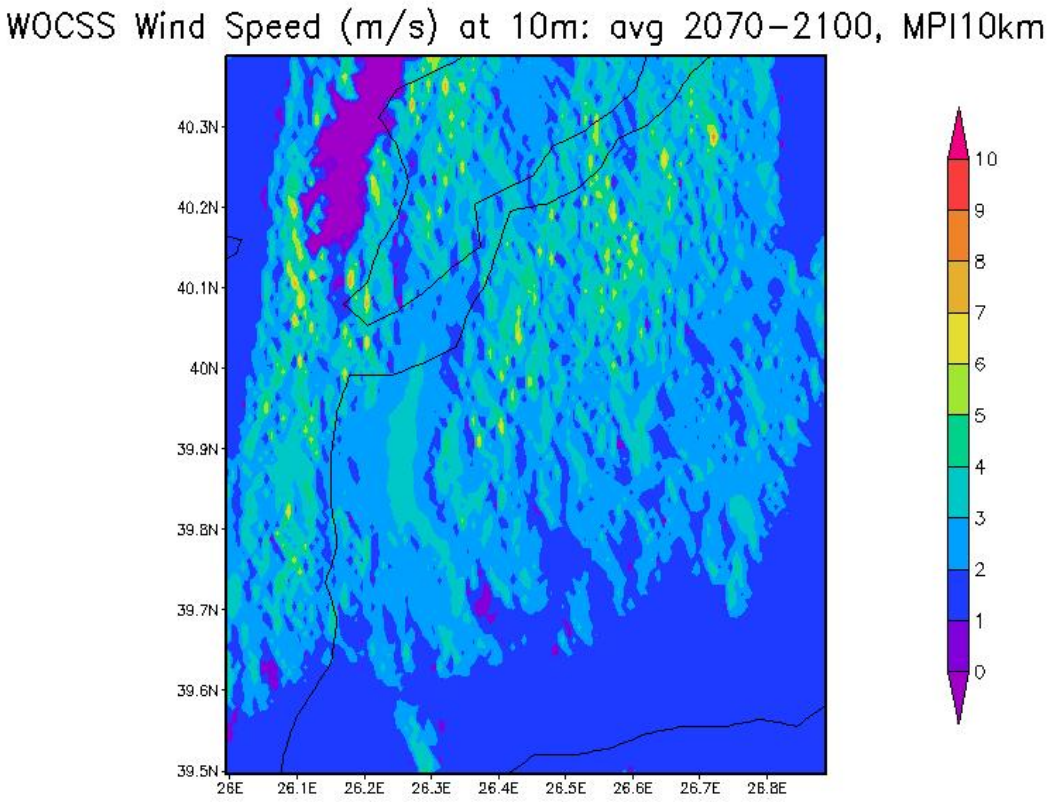

Figure 3.14: WOCSS wind speed (m/s) result at 10m: avg of 2070-2100

At Figure 3.14, for the average of the period of 2070-2100 at 10m height, maximum wind speed is about 8.5 m/s and this is 0.65 m/s more than the average of the period of 2040-2070 at 10m height.

3.4.2. Wind Direction at 10 meters

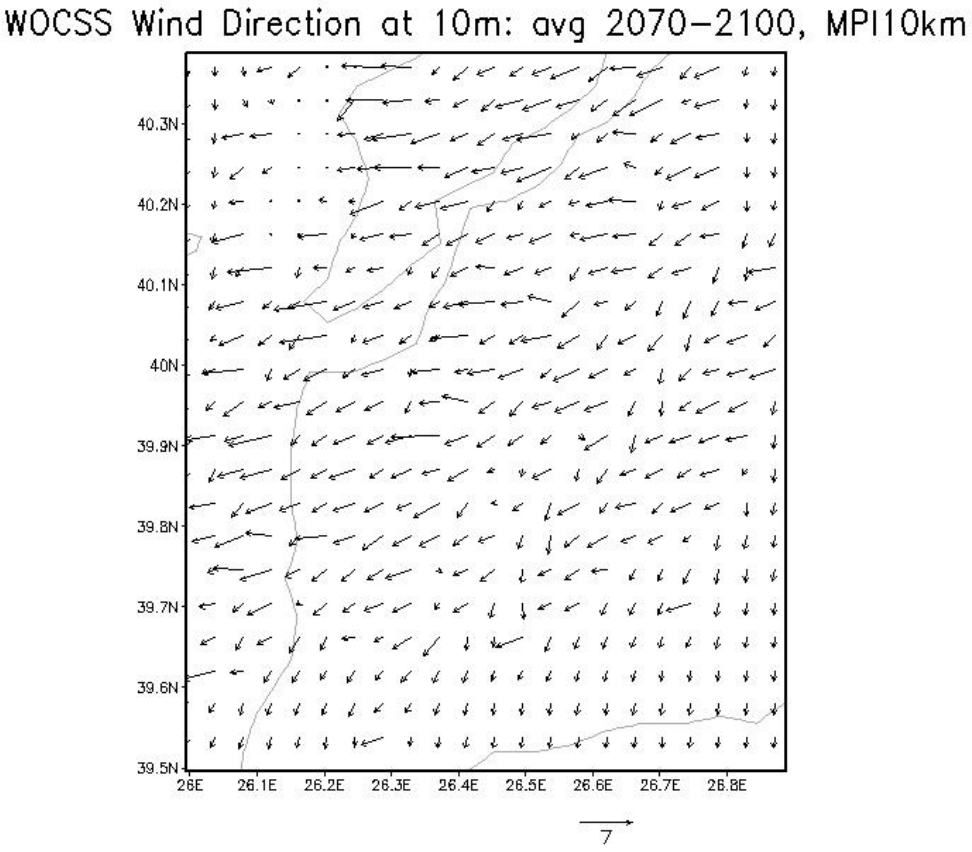

Figure 3.15: WOCSS wind direction result at 10m: avg of 2070-2100

At Figure 3.15, for the average of the period of 2070-2100 at 10m height, the high-speed wind is distributed around the bosporus and the north and the northwest of the region.

3.4.3. Wind Speed at 50 meters

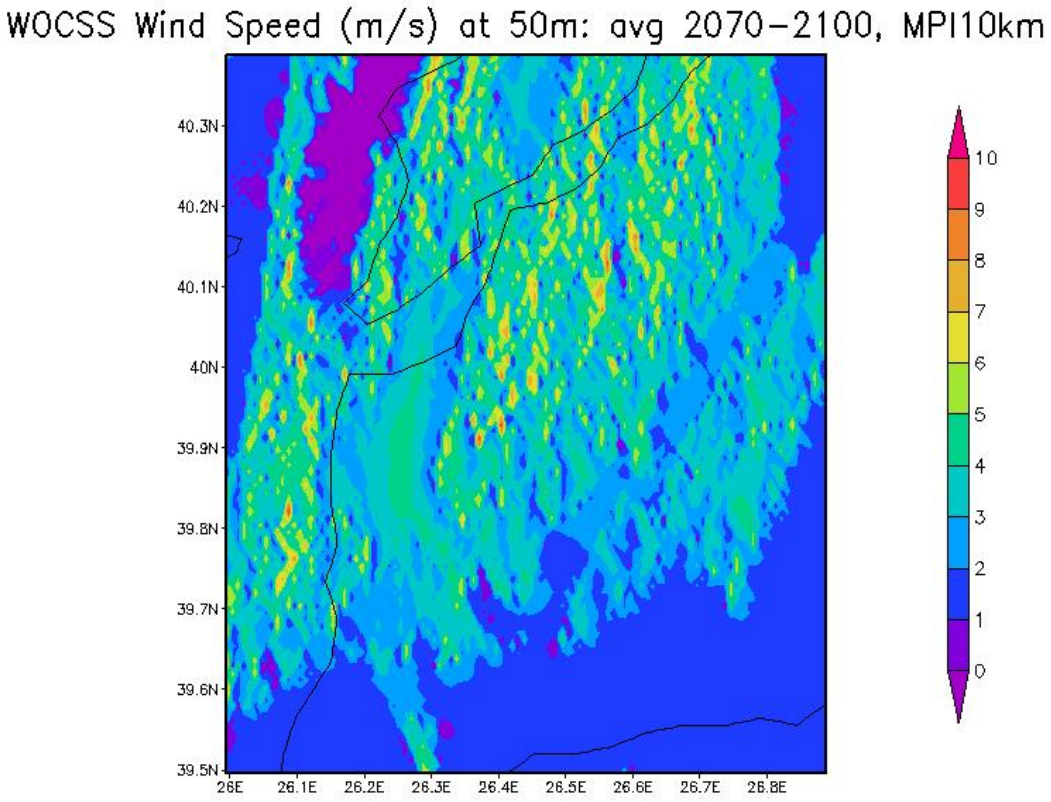

Figure 3.16: WOCSS wind speed (m/s) result at 50m: avg of 2070-2100

At Figure 3.16, for the average of the period of 2070-2100 at 50m height, maximum wind speed is about 9.81 m/s and this is 1.31 m/s more than at 10m height at this time period and this is 0.81 m/s more than the average of the period of 2040-2070 at 50m height. And this maximum wind speed is 1.73 m/s more than the average of the period of 2010-2040 at 50m height. This difference is so important, because, after 2070, we expect strong winds on Canakkale Biga region. These strong winds maybe cause some extreme events at this region.

3.4.4. Wind Direction at 50 meters

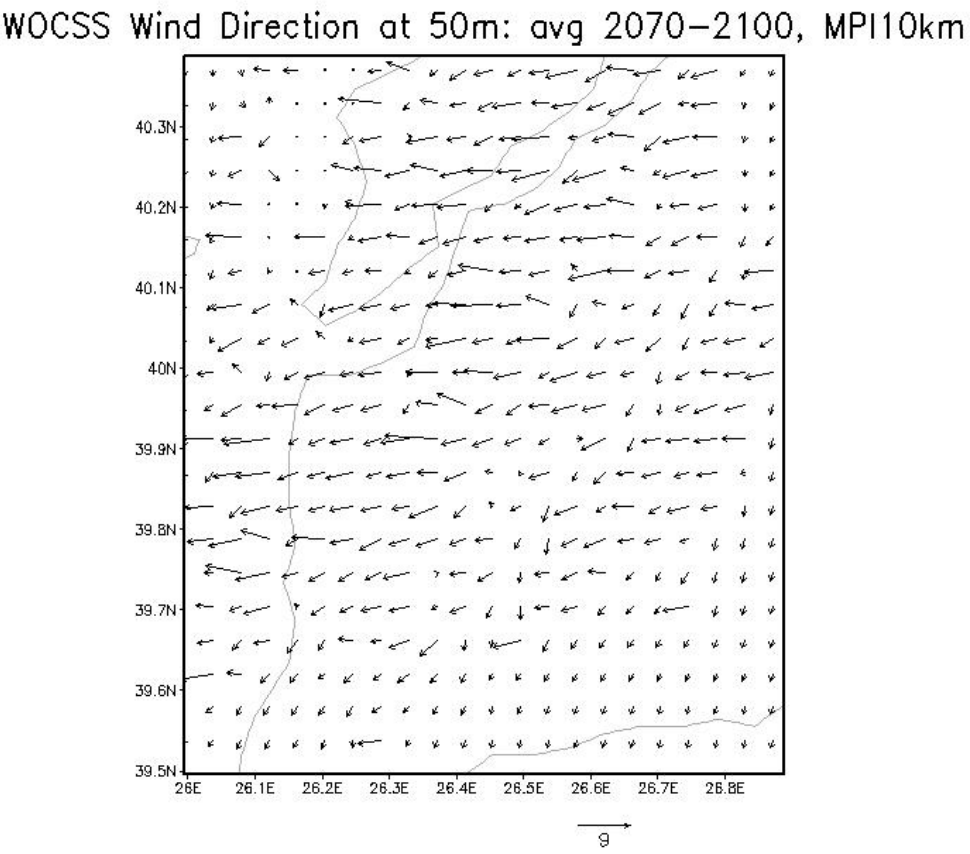

Figure 3.17: WOCSS wind direction result at 50m: avg of 2070-2100

At Figure 3.17, for the average of the period of 2070-2100 at 50m height, the high-speed wind is distributed around the bosporus and the north the of the region.

3.5. Wind Speed Change at 10 meters of all time periods

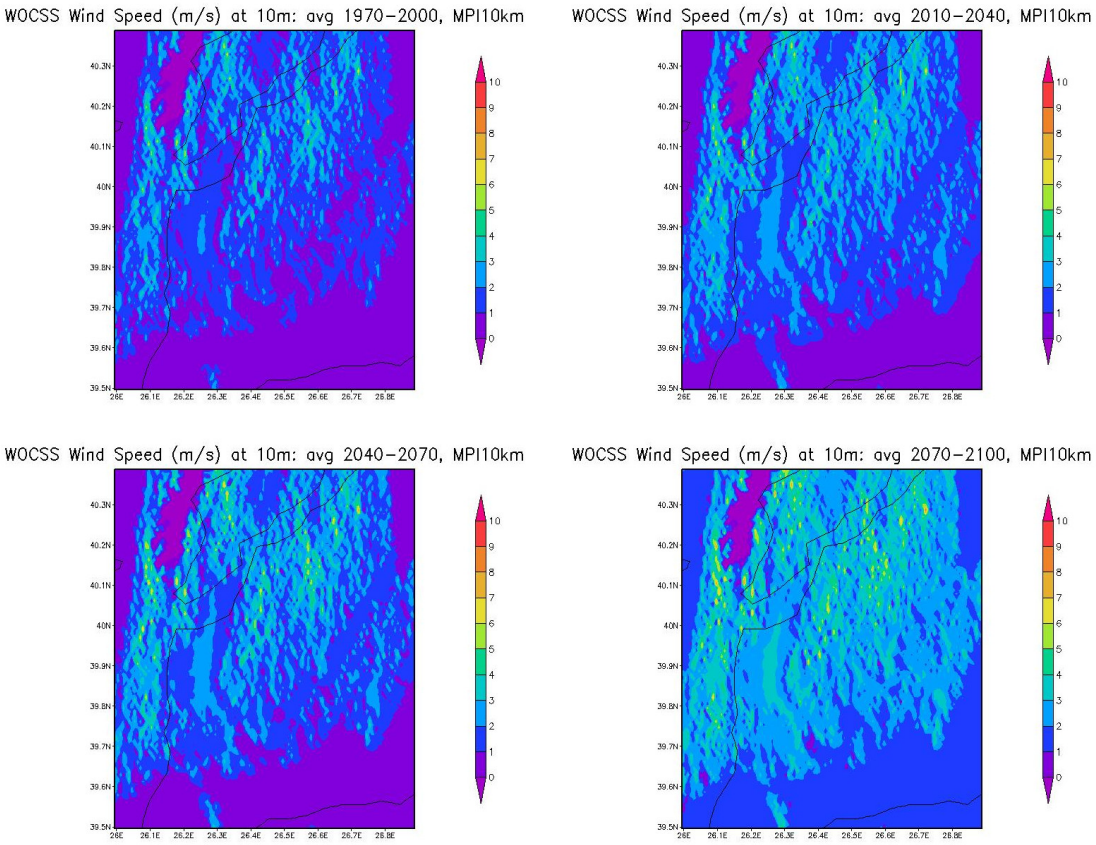

Figure 3.18: Wind speed (m/s) results at 10m

At Figure 3.18, at 10m height, maximum speed of the wind of the periods of 1970-2000 is 6.69 m/s, 2010-2040 is 7.0 m/s, 2040-2070 is 7.85 m/s and 2070-2100 is 8.5 m/s. As seen from the results, wind speed will increase at the future.

3.6. Wind Direction Change at 10 meters of all time periods

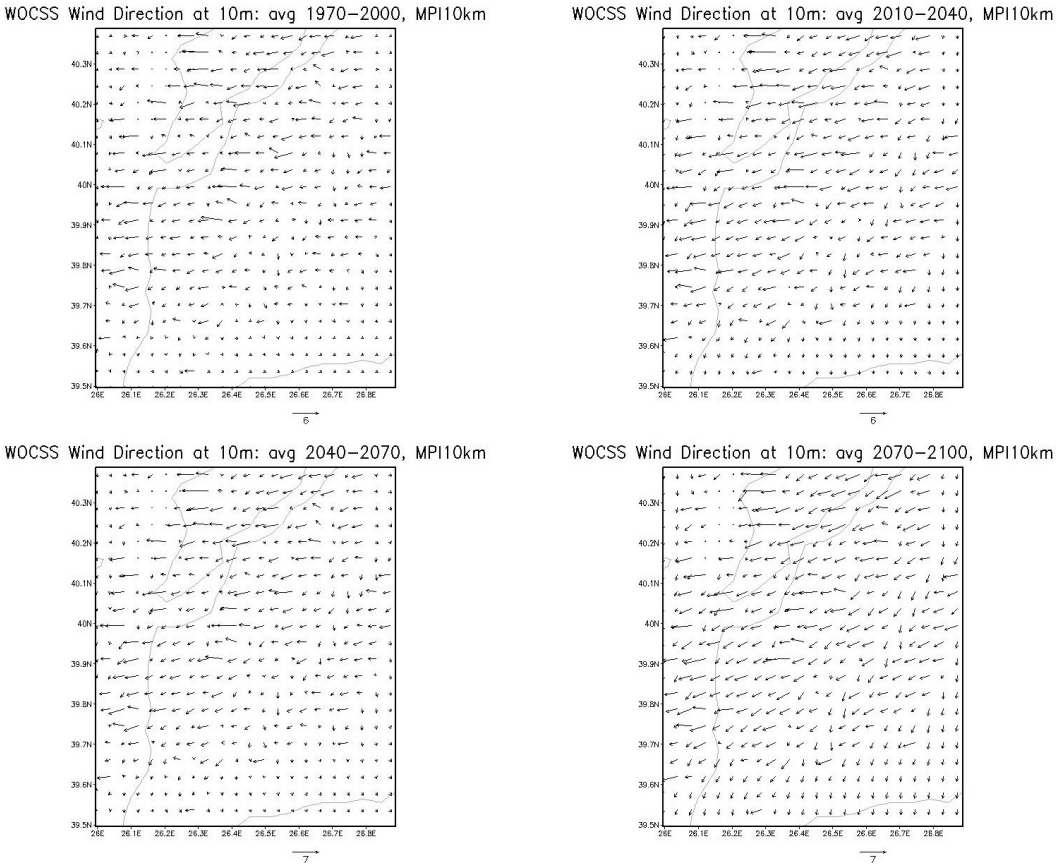

Figure 3.19: Wind direction results at 10m

At Figure 3.19, at 10m height, the high-speed wind is distributed around the bosporus and north of the region for all the time periods.

3.7. Wind Speed Change at 50 meters of all time periods

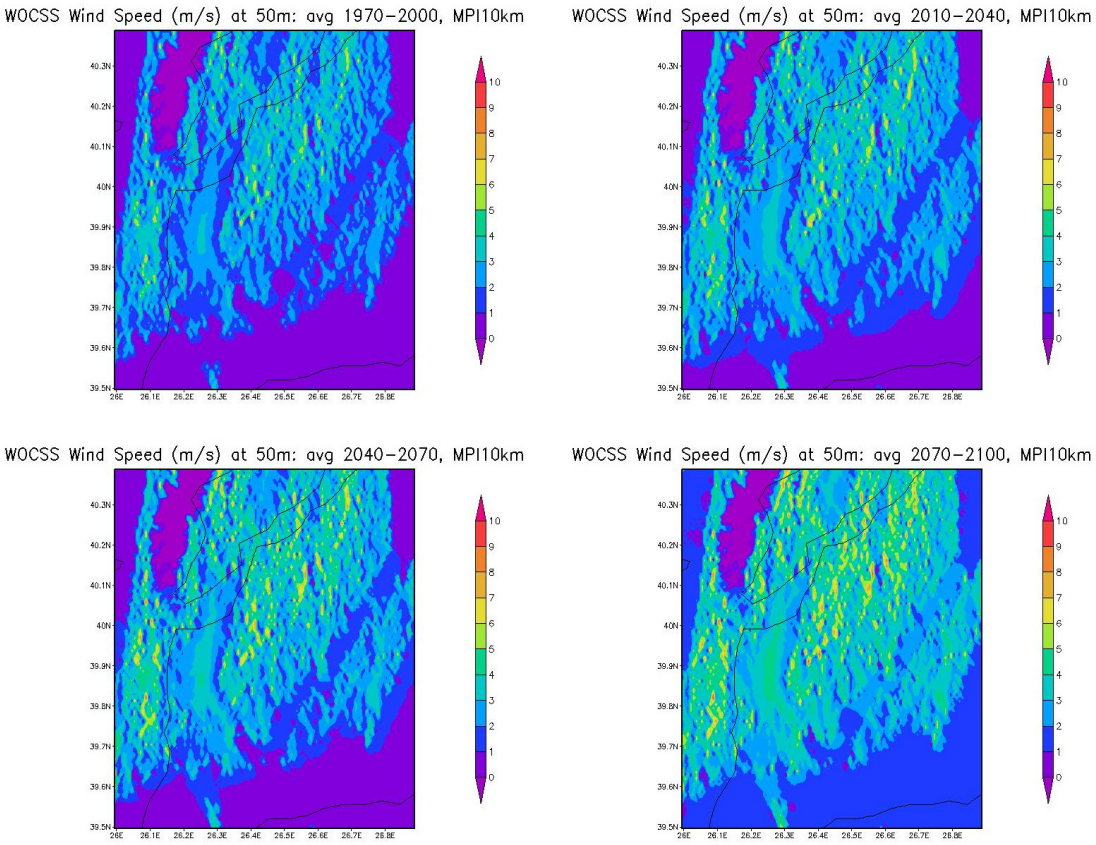

Figure 3.20: Wind (m/s) results at 50m

At Figure 3.20, at 50m height, maximum speed of the wind of the periods of 1970-2000 is 7.69 m/s, 2010-2040 is 8.08 m/s, 2040-2070 is 9.0 m/s and 2070-2100 is 9.81 m/s. As seen from the results, wind speed will increase at the future.

3.8. Wind Direction Change at 50 meters of all time periods

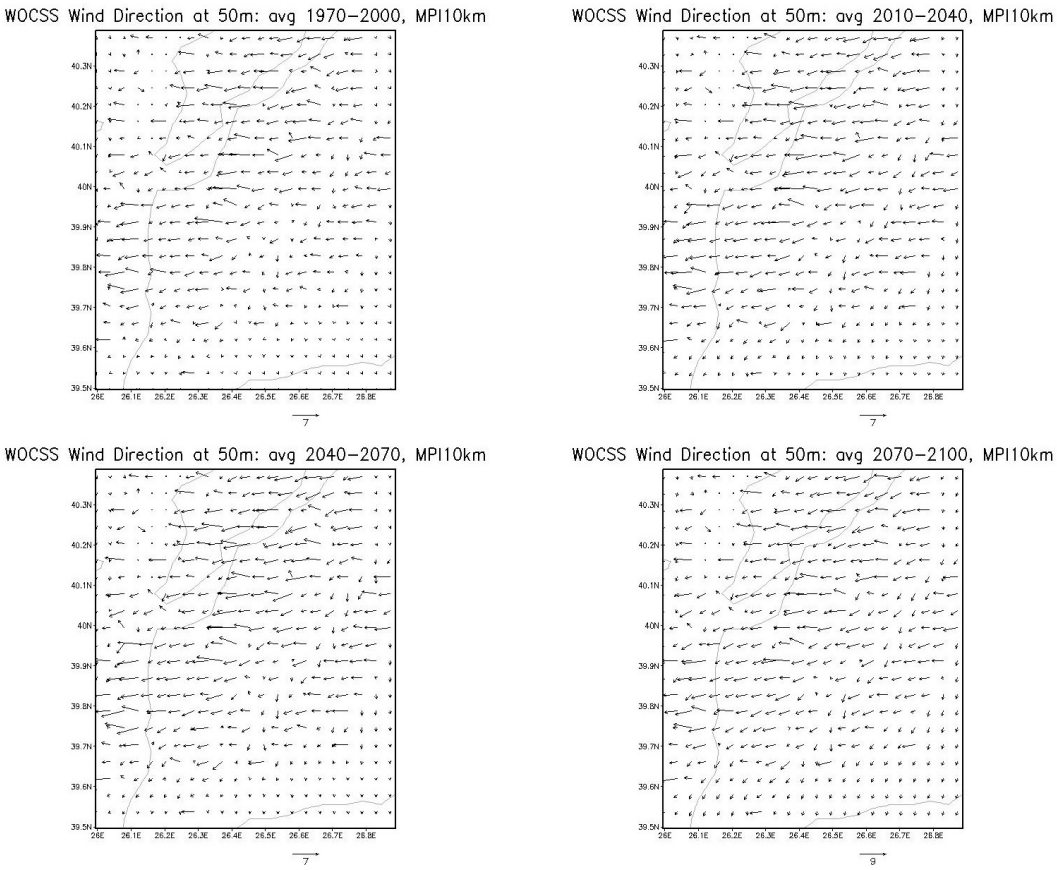

Figure 3.21: Wind direction results at 50m

At Figure 3.21, at 50m height, the high-speed wind is distributed around the bosporus and north and northwest of the region for all the time periods.

4. CONCLUSION

4.1. Conclusion

This study aims to demonstrate the change in wind direction and speed for the time periods of 1970-2000, 2010-2040, 2040-2070, and 2070-2100 according to the climate change. In this study, rather than observed data, simulated data from RegCM4 were used to simulate wind direction and speed using WOCSS.

For this case study, Canakkale Biga region is selected because of the high wind potential in Turkey. According to the Turkey Wind Map from General Directorate of Meteorology of Turkey, Canakkale has the range of 6.5 m/s to 7.5 m/s wind speed at 50m height.

Table 4.1: Results of Wind Speed of All Time Periods

Height	**1970-2000**	**2010-2040**	**2040-2070**	**2070-2100**
10 meters	6.69 m/s	7.0 m/s	7.85 m/s	8.5 m/s
50 meters	7.69 m/s	8.08 m/s	9.0 m/s	9.81 m/s

As seen at the Table 4.1, it is obvious that at the same time period, there is a difference between 10m and 50m maximum wind speed and this value is at least 1.0 m/s. Wind direction and speed distribution indicate changes between 10m and 50m altitude.

For the different time periods, it has seen at Table 4.1 that wind speed is more than previous time periods for 10m and 50m altitudes. This is the most important point of this study, because when we look at the wind power plants' available speed of hub engines, they have a rage to generate electricity. To illustrate, some hub

engines work with the range of 5 m/s to 7 m/s and when the wind speed exceeds 7 m/s, hub engine stops automatically. For this reason, at least for the next thirty years, at least 0.5 m/s is a big increase for middle hub engines, especially, the region of Canakkale Biga region, so it is more important to choose the right hub engine for specific areas according to the climate change.

WOCSS is a good option for determining wind direction and speed at 1 km resolution, especially, WOCSS needs low computer power and storage capacity. Rather than RegCM4, which needs more computer power and more storage capacity to get simulated wind direction and speed data at 1 km resolution and it is not available at this moment, WOCSS is faster. Last but not least, WOCSS is based on Fortran and it is, also open source.

4.2. Future work

After this study, my next goal is to compare between the more results of WOCSS and RegCM4 at 1km resolution with the help of ICTP for this time period or more.

REFERENCES

1. "Wind Energy Worldwide", http://www.wwindea.org/the-world-sets-new-wind-installations-record-637-gw-new-capacity-in-2015/, accessed at June 2016.

2. Giorgi, F., E. Coppola, F. Solmon, L. Mariotti, M. B. Sylla, X. Bi, N. Elguindi, G. T. Diro, V. Nair, G. Giuliani, U. U. Turuncoglu, S. Cozzini, I. Güttler, T. A. O'Brien, A. B. Tawfik, A. Shalaby, A. S. Zakey, A. L. Steiner, F. Storda, L. C. Sloan and C. Brankovic, "RegCM4: model description and preliminary tests over multiple CORDEX domains", *Climate Research*, Vol. 52, pp. 7–29, 2012.

3. Ludwig, F. L., J. M. Livingston and R. M. Endlich, "Use of Mass Conservation and Critical Dividing Streamline Concepts for Efficient Objective Analysis of Winds in Compex Terrain", *Journal of Applied Meteorology*, Vol. 30, p. 1490, 1991.

4. "Meteoroloji Genel Müdürlüğü Rüzgar Atlası", http://www.mgm.gov.tr/arastirma/yenilenebilir-enerji.aspx?s=ruzgaratlasi, accessed at May 2016.

5. Bridger, A. F. C., A. J. Becker, F. L. Ludwig and R. M. Endlich, "Evaluation of the WOCSS Wind Analysis Scheme for the San Francisco Bay Area", *Journal of Applied Meteorology*, Vol. 33, p. 1210, 1994.

6. Ludwig, F. L., *A Guide To The Winds On Critical Streamline Surfaces (WOCSS) Code, Salt Lake City Area Data And Other Related Files*, 1995.

7. Ludwig, F. L. and D. Sinton, "Evaluating an Objective Wind Analysis Technique with a Long Record of Routinely Collected Data", *Journal of Applied Meteorology*, Vol. 39, pp. 335–348, 2000.

8. Ludwig, F. L., D. K. Miller and S. G. Gallaher, "Evaluating a hybrid prognostic-diagnostic model that improves wind forecast resolution in complex coastal topography", *Journal of Applied Meteorology and Climatology*, Vol. 45, pp. 155–177, 2006.

9. Vesecky, J. F., J. Drake, K. Laws, F. L. Ludwig, C. C. Teague, J. D. Paduan and D. Sinton, "Coastal eddies in the ocean wind field as observed by single and multifrequency HF radars on monterey bay, california", *OCEANS 2007 - EUROPE*, Vol. 1–3, pp. 1123–1127, 2007.

10. Karaman, G. and K. Aksay, "Natural Gas And Wind Based Cycle Plants In Supplying The Needs Of Energy; A Strategic Analysis On The Investments", *The Journal of Global Engineering Studies*, Vol. 2, pp. 9–35, 2015.

11. "METOFFICE", http://www.metoffice.gov.uk/climate-guide/climate-change, accessed at June 2016.

12. "NASA", http://www.nasa.gov/audience/forstudents/k-4/stories/nasa-knows/what-is-climate-change-k4.html, accessed at June 2016.

13. *IPCC Fifth Assessment Report: Climate Change 2014 Synthesis Report*, 2014.

14. "RCP Scenarios", https://en.wikipedia.org/wiki/Representative_Concentration_Pathways, accessed at May 2016.

15. van Vuuren, D. P., J. Edmonds, M. Kainuma, K. Riahi, A. Thomson, K. Hibbard, G. C. Hurtt, T. Kram, V. Krey, J.-F. Lamarque, T. Masui, M. Meinshausen, N. Nakicenovic, S. J. Smith and S. K. Rose, "The representative concentration pathways: an overview", Vol. 109, pp. 5–31, 2011.

16. Riahi, K., A. Grübler and N. Nakicenovica, "Scenarios of long-term socio-economic and environmental development under climate stabilization", *Else-*

vier, Vol. 74, pp. 887–935, 2007.

17. Rao, S. and K. Riahi, "The Role of Non-CO_3 Greenhouse Gases in Climate Change Mitigation: Long-term Scenarios for the 21st Century", *The Energy Journal*, Vol. 27, pp. 177–200, 2006.

18. Fujino, J., R. Nair, M. Kainuma, T. Masui and Y. Matsuoka, "Multi-gas Mitigation Analysis on Stabilization Scenarios Using Aim Global Model", *The Energy Journal*, Vol. 27, pp. 343–353, 2006.

19. Hijioka, Y., Y. Matsuoka, H. Nishimoto, M. Masui and M. Kainuma, "Global GHG emissions scenarios under GHG concentration stabilization targets", *Journal of Global Environmental Engineering*, Vol. 13, pp. 97–108, 2008.

20. Smith, S. J. and T. Wigley, "Multi-Gas Forcing Stabilization with Minicam", *The Energy Journal*, Vol. 27, pp. 373–391, 2006.

21. Clarke, L., J. Edmonds, H. Jacoby, H. Pitcher, J. Reilly and R. Richels, *Scenarios of Greenhouse Gas Emissions and Atmospheric Concentrations*, U.S. Climate Change Science Program and the Subcommittee on Global Change Research. Department of Energy, Office of Biological and Environmental Research, 2007.

22. Wise, M., K. Calvin, A. Thomson, L. Clarke, B. Bond-Lamberty, R. Sands, S. J. Smith, A. Janetos and J. Edmonds, "Implications of Limiting CO2 Concentrations for Land Use and Energy", *Science*, Vol. 324, pp. 1183–1186, 2009.

23. van Vuuren, D., B. Eickhout, P. Lucas and M. den Elzen, "Long-Term Multi-Gas Scenarios to Stabilise Radiative Forcing — Exploring Costs and Benefits Within an Integrated Assessment Framework", *The Energy Journal*, Vol. 27, pp. 201–233, 2006.

24. van Vuuren, D. P., M. J. G. den Elzen, P. L. Lucas, B. Eickhout, B. J. Strengers, B. van Ruijven, S. Wonink and R. van Houdt, "Stabilizing greenhouse gas concentrations at low levels: an assessment of reduction strategies and costs", *Climatic Change*, Vol. 81, pp. 119–159, 2007.

25. Riahi, K., S. Rao, V. Krey, C. Cho, V. Chirkov, G. Fischer, G. Kindermann, N. Nakicenovic and P. Rafaj, "RCP 8.5 - A scenario of comparatively high greenhouse gas emissions", *Climatic Change*, Vol. 109, pp. 33–57, 2011.

26. "General Circulation Models", http://climate.calcommons.org/lists/general-circulation-models, accessed at May 2016.

27. "Regional Climate Model", http://glossary.ametsoc.org/wiki/Regional_climate_model, accessed at May 2016.

28. "RegCM4", https://www.ictp.it/research/esp/models/regcm4.aspx, accessed at June 2016.

29. Elguindi, N., X. Bi, F. Giorgi, B. Nagarajan, J. Pal, F. Solmon, S. Rauscher, A. Zakey, T. O'Brien, R. Nogherotto and G. Giuliani, *Regional Climate Model RegCM Reference Manual Version 4.5*, ICTP, 2014.

30. "ERAINTERIM", http://www.ecmwf.int/en/research/climate-reanalysis/era-interim, accessed at June 2016.

31. Kitada, T., A. Kaki, H. Ueda and L. K. Peters, "Estimation of vertical air motion from limited horizontal wind data—a numerical experiment", *Atmospheric Environment*, Vol. 17, pp. 2181–2192, 1983.

32. Bayraktar, E., *Terrain Induced Wind Profiles*, Master's Thesis, Bogazici University, 2003.

33. Fadillioglu, C., I. C. Kiyisuren and C. E. Ayhan, *Wind Power Production System Design*, Bogazici University, 2016.

APPENDIX A: MATLAB CODES

```
function [x,y,utmzone] = deg2utm(Lat,Lon)
% [x,y,utmzone] = deg2utm(Lat,Lon)
% Description: Function to convert lat/lon vectors into UTM coordinates (WGS84).
% Some code has been extracted from UTM.m function by Gabriel Ruiz Martinez.
% Inputs:
% Lat: Latitude vector. Degrees. +ddd.ddddd WGS84
% Lon: Longitude vector. Degrees. +ddd.ddddd WGS84
% Outputs:
% x, y , utmzone. See example
% Example 1:
% Lat=[40.3154333; 46.283900; 37.577833; 28.645650; 38.855550; 25.061783];
% Lon=[-3.4857166; 7.8012333; -119.95525; -17.759533; -94.7990166; 121.640266];
% [x,y,utmzone] = deg2utm(Lat,Lon);
% fprintf('%7.0f ',x)
% 458731 407653 239027 230253 343898 362850
% fprintf('%7.0f ',y)
% 4462881 5126290 4163083 3171843 4302285 2772478
% utmzone = 30 T 32 T 11 S 28 R 15 S 51 R
% Example 2: If you have Lat/Lon coordinates in Degrees, Minutes and Seconds
% LatDMS=[40 18 55.56; 46 17 2.04];
% LonDMS=[-3 29 8.58; 7 48 4.44];
% Lat=dms2deg(mat2dms(LatDMS)); %convert into degrees
% Lon=dms2deg(mat2dms(LonDMS)); %convert into degrees
% [x,y,utmzone] = deg2utm(Lat,Lon)
% Author:
% Rafael Palacios
% Universidad Pontificia Comillas Madrid, Spain
% Version: Apr/06, Jun/06, Aug/06, Aug/06
% Aug/06: fixed a problem (found by Rodolphe Dewarrat) related to southern
% hemisphere coordinates.
% Aug/06: corrected m-Lint warnings
% Argument checking
error(nargchk(2, 2, nargin)); %2 arguments required
n1=length(Lat); n2=length(Lon);
if (n1~=n2)
error('Lat and Lon vectors should have the same length');
end
% Memory pre-allocation
x=zeros(n1,1); y=zeros(n1,1); utmzone(n1,:)='60 X';
% Main Loop
for i=1:n1
la=Lat(i); lo=Lon(i); sa = 6378137.000000 ; sb = 6356752.314245;
%e = ( ( ( sa ^ 2 ) - ( sb ^ 2 ) ) ^ 0.5 ) / sa;
e2 = ( ( ( sa ^ 2 ) - ( sb ^ 2 ) ) ^ 0.5 ) / sb; e2cuadrada = e2 ^ 2; c = ( sa ^ 2 ) / sb;
%alpha = ( sa - sb ) / sa;  %f
%ablandamiento = 1 / alpha; % 1/f
lat = la * ( pi / 180 ); lon = lo * ( pi / 180 );
Huso = fix( ( lo / 6 ) + 31); S = ( ( Huso * 6 ) - 183 ); deltaS = lon - ( S * ( pi / 180 ) );
```

Figure A.1: deg2utm.m

```
if (la<-72), Letra='C';
elseif (la<-64), Letra='D';
elseif (la<-56), Letra='E';
elseif (la<-48), Letra='F';
elseif (la<-40), Letra='G';
elseif (la<-32), Letra='H';
elseif (la<-24), Letra='J';
elseif (la<-16), Letra='K';
elseif (la<-8), Letra='L';
elseif (la<0), Letra='M';
elseif (la<8), Letra='N';
elseif (la<16), Letra='P';
elseif (la<24), Letra='Q';
elseif (la<32), Letra='R';
elseif (la<40), Letra='S';
elseif (la<48), Letra='T';
elseif (la<56), Letra='U';
elseif (la<64), Letra='V';
elseif (la<72), Letra='W';
else Letra='X';
end
a = cos(lat) * sin(deltaS); epsilon = 0.5 * log( ( 1 + a) / ( 1 - a ) );
nu = atan( tan(lat) / cos(deltaS) ) - lat;
v = ( c / ( ( 1 + ( e2cuadrada * ( cos(lat) ) ^ 2 ) ) ) ^ 0.5 ) * 0.9996;
ta = ( e2cuadrada / 2 ) * epsilon ^ 2 * ( cos(lat) ) ^ 2; a1 = sin( 2 * lat );
a2 = a1 * ( cos(lat) ) ^ 2; j2 = lat + ( a1 / 2 ); j4 = ( ( 3 * j2 ) + a2 ) / 4;
j6 = ( ( 5 * j4 ) + ( a2 * ( cos(lat) ) ^ 2) ) / 3; alfa = ( 3 / 4 ) * e2cuadrada;
beta = ( 5 / 3 ) * alfa ^ 2; gama = ( 35 / 27 ) * alfa ^ 3;
Bm = 0.9996 * c * ( lat - alfa * j2 + beta * j4 - gama * j6 );
xx = epsilon * v * ( 1 + ( ta / 3 ) ) + 500000; yy = nu * v * ( 1 + ta ) + Bm;
if (yy<0)
yy=9999999+yy;
end
x(i)=xx; y(i)=yy; utmzone(i,:)=sprintf('%02d %c',Huso,Letra);
end
```

Figure A.1: deg2utm.m (cont.)

```
[canakkale1, refvec] = dted('4026', 3,[40 40.5],[26.0 27.0]);
[canakkale2, refvec] = dted('3926', 3,[39.5 40.0],[26.0 27.0]);
canakkale90=vertcat(canakkale2,canakkale1);
[canakkale1_990, refvec] = dted('4026', 33,[40 40.5],[26.0 27.0]);
[canakkale2_990, refvec] = dted('3926', 33,[39.5 40.0],[26.0 27.0]);
canakkale990=vertcat(canakkale2_990,canakkale1_990);
for i=1:108
for j=1:108
canak990(i,j)=canakkale990(i+2,j);
end
end
```

Figure A.2: Locate Topo.m

```
%This script developed by Kamil Collu.
%This script creates needed excel file for WOCSS use.
%Before using this script, create coordinates.xlsx file.
%Before using this script, check the folder paths.
%Reading RegCM output data

%In this section, script reads normal (surface) data
%normal data
psnormal=load('/media/username/NewVolume/Dropbox/output/ERAINT/2010-2040/normal/psall.csv');
tsnormal=load('/media/username/NewVolume/Dropbox/output/ERAINT/2010-2040/normal/tsall.csv');
uanormal=load('/media/username/NewVolume/Dropbox/output/ERAINT/2010-2040/normal/uaall.csv');
vanormal=load('/media/username/NewVolume/Dropbox/output/ERAINT/2010-2040/normal/vaall.csv');

%In this section, script reads 10 meters height data (from radiosonde)
%10m data
ps10m=csvread('/media/username/NewVolume/Dropbox/output/ERAINT/2010-2040/tsonde/10m/ps.csv',1,0);
ts10m=csvread('/media/username/NewVolume/Dropbox/output/ERAINT/2010-2040/tsonde/10m/ts.csv',1,0);
ua10m=csvread('/media/username/NewVolume/Dropbox/output/ERAINT/2010-2040/tsonde/10m/ua.csv',1,0);
va10m=csvread('/media/username/NewVolume/Dropbox/output/ERAINT/2010-2040/tsonde/10m/va.csv',1,0);

%In this section, script reads radiosonde data (except 10 meters)
%tsonde data
hgtsonde=load('/media/username/NewVolume/Dropbox/output/ERAINT/2010-2040/tsonde/hgtall.csv');
tasonde=load('/media/username/NewVolume/Dropbox/output/ERAINT/2010-2040/tsonde/taall.csv');
uasonde=load('/media/username/NewVolume/Dropbox/output/ERAINT/2010-2040/tsonde/uaall.csv');
vasonde=load('/media/username/NewVolume/Dropbox/output/ERAINT/2010-2040/tsonde/vaall.csv');

%Writing excel file

% value

filename = 'canakkale2010-2040.xls';
sheet = 1;
psn = [psnormal];
tsn = [tsnormal];
uan = [uanormal];
van = [vanormal];
ps10 = [ps10m];
ts10 = [ts10m];
ua10 = [ua10m];
va10 = [va10m];
hgtso = [hgtsonde];
taso = [tasonde];
uaso = [uasonde];
vaso = [vasonde];

xlwrite(filename,psn,sheet,'C3'); %ps normal data
xlwrite(filename,tsn,sheet,'D3'); %ts normal data
xlwrite(filename,uan,sheet,'E3'); %ua normal data
xlwrite(filename,van,sheet,'F3'); %va normal data
xlwrite(filename,ps10,sheet,'K3'); %ps 10m data
xlwrite(filename,ts10,sheet,'M3'); %ts 10m data
xlwrite(filename,ua10,sheet,'N3'); %ua 10m data
xlwrite(filename,va10,sheet,'O3'); %ua 10m data
xlwrite(filename,hgtso,sheet,'L4'); %hgt sonde data
xlwrite(filename,taso,sheet,'M4'); %ta sonde data
xlwrite(filename,uaso,sheet,'N4'); %ua sonde data
xlwrite(filename,vaso,sheet,'O4'); %va sonde data
```

Figure A.3: createexcel.m

```
clear all

%coordinates

latcoord=xlsread('/media/username/NewVolume/Dropbox/output/ERAINT/2010-2040/coordinates.xlsx','A2:A21');
loncoord=xlsread('/media/username/NewVolume/Dropbox/output/ERAINT/2010-2040/coordinates.xlsx','B2:B21');
lattsonde=xlsread('/media/username/NewVolume/Dropbox/output/ERAINT/2010-2040/coordinates.xlsx',1,'D3');
lontsonde=xlsread('/media/username/NewVolume/Dropbox/output/ERAINT/2010-2040/coordinates.xlsx',1,'E3');
zvalues=xlsread('/media/username/NewVolume/Dropbox/output/ERAINT/2010-2040/coordinates.xlsx','G3:G13');
pressvalues=xlsread('/media/username/NewVolume/Dropbox/output/ERAINT/2010-2040/coordinates.xlsx','H3:H13');

filename = 'canakkale2010-2040.xls';
A3lat = [latcoord];
B3lon = [loncoord];
D3lat = [lattsonde];
E3lon = [lontsonde];
J4z = [zvalues]; %tsonde z values (constant)
K4p = [pressvalues]; %tsonde Regcm4 pressure level values (constant)
sheet = 1;
xlwrite(filename,A3lat,sheet,'A3');
xlwrite(filename,B3lon,sheet,'B3');
xlwrite(filename,D3lat,sheet,'H4');
xlwrite(filename,E3lon,sheet,'I4');
xlwrite(filename,J4z,sheet,'J4');
xlwrite(filename,K4p,sheet,'K4');

clear all;

%Excel titles

filename = 'canakkale2010-2040.xls';
C1 = {'Data of chosen station points'};
A2 = {'Lat(decdeg)','Lon(decdeg)','pressure(mb)','temp(K)','wind-u(m/s)','wind-v(m/s)',NaN}
A9 = {'T-sonde coordinates',NaN,'z','pressure(mb)','height(m)','temp(K)','wind-u(m/s)','wind-v(m/s)',NaN}
A18= {'Hour','Day','Month','Year'};
K1 = {'Data of chosen t-sonde point'};
Q1 = {'Date (has no effect on calculations)'};
H3 = {'Lat(decdeg)','Lon(decdeg)'};
J3 = (0);
L3 = (10); %10m (constant)
Q3 = [20,17,5,2016]; %default Date Hour value (you can change if you want)
P3 = NaN; %correction

sheet = 1;
xlwrite(filename,C1,sheet,'C1');
xlwrite(filename,A2,sheet,'A2');
xlwrite(filename,K1,sheet,'K1');
xlwrite(filename,Q1,sheet,'Q1');
xlwrite(filename,H3,sheet,'H3');
xlwrite(filename,J3,sheet,'J3');
xlwrite(filename,L3,sheet,'L3');
xlwrite(filename,Q3,sheet,'Q3');
xlwrite(filename,P3,sheet,'P3');

clear all;
```

Figure A.3: createexcel.m (cont.)

```
%This script developed by Cagla Fadillioglu, Ihsan Cagatay Kiyisuren.
%This script prepares necessary files for the first run of 'wocss'
%Files will appear in the '1st' directory and be ready to be used directly with wocss
%Directories should be created by the user in the following form before
%running the script
%.../place/date/'1st'
%After creating them,user should put the necessary excel file to:
%.../place/date/
%and the necessary topography file to:
%.../place/
%----This part should be changed by the user if necessary----
place='canakkale'; %directory name (at the same time the name of the working area)
date='2010-2040'; %date that the data belongs to (does not affect the outputs)
filename ='canakkale2010-2040.xlsx'; %name of the excel file in which the full regcm data is written
topographyfile='biga990.dat'; %topography file that will be used for the first run
corner1NS=39.5; %southwest corner N-S
corner1EW=26.0; %southwest corner E-W
corner2NS=40.4; %northeast corner N-S
corner2EW=26.9; %northeast corner E-W
subfolder='1st'; %folder for the first run
filename2='winds.dat'; %this file will be created in the ('%s',subfolder) directory after running the script
filename3='terrain.dat'; %this file will be created in the ('%s',subfolder) directory after running the script
filename4='rundat.dat'; %this file will be created in the ('%s',subfolder) directory after running the script
conversion1=1; %choose 1 for (m/s), choose 0 for (knot)
conversion2=1; %choose 1 for (m), choose 0 for (feet)
gridsize=0.99; %don't change if you would like to use that script
gridx=108; %grid size in x-coordinate for wocss-first run (NCRS in wocss)
gridy=108; %grid size in y-coordinate for wocss-first run (MCRS in wocss)
%directories are identified
fullname1=fullfile(place,date,filename); fullname2=fullfile(place,date,subfolder,filename2);
fullname3=fullfile(place,topographyfile); fullname4=fullfile(place,date,subfolder,filename3);
fullname5=fullfile(place,date,subfolder,filename4);
%file id's are determined according to the permission
%'r' for read, 'w' for write
fid= fopen(fullname2, 'w'); fid2=fopen(fullname3, 'r'); fid3=fopen(fullname4, 'w');
fid4=fopen(fullname5, 'w');
%utm conversion for the corner points
[corner1utmx,corner1utmy,corner1zone]=deg2utm(corner1NS,corner1EW);
corner1utmx=corner1utmx*10^-3; corner1utmy=corner1utmy*10^-3;
[corner2utmx,corner2utmy,corner2zone]=deg2utm(corner2NS,corner2EW);
corner2utmx=corner2utmx*10^-3; corner2utmy=corner2utmy*10^-3;
format='%f'; %scan format
terrain=fscanf(fid2,format); %topography file is scanned
%excel file is scanned and data is read with corresponding excel cell ranges
xlRange = 'Q3:T3'; %reads date of the data
date = xlsread(fullname1,xlRange);
xlRange = 'A3:A100'; %reads latitude coordinates of the station points
Lat = xlsread(fullname1,xlRange);
xlRange = 'B3:B100'; %reads longitude coordinates of the station points
Lon = xlsread(fullname1,xlRange);
station=length(Lon); %calculates number of stations
xlRange = 'C3:C100'; %reads pressure values of the station points
press = xlsread(fullname1,xlRange);
xlRange = 'D3:D100'; %reads temperature values of the station points
temp = xlsread(fullname1,xlRange)-273.1;
xlRange = 'E3:E100'; %reads u components of the velocity for the station points
ucomp = xlsread(fullname1,xlRange);
xlRange = 'F3:F100'; %reads v components of the velocity for the station points
```

Figure A.4: wocss.m

```
vcomp = xlsread(fullname1,xlRange);
speed=sqrt(ucomp.^2+vcomp.^2); %calculates wind speed
dire=180+atan2(ucomp,vcomp)*(180/pi); %calculates wind direction
for i=1:station
if (dire(i) > 360)
dire(i)= dire(i)-360;
end
end
[x,y,utmzone] = deg2utm(Lat,Lon); %makes utm conversion for the station points
%writes data to the created winds.dat file
fprintf(fid,'%d %d %d %d \n \n',date(1:4)); %writes date
fprintf(fid,'6 0 0 0 0 \n \n'); %writes necessary numbers for wocss
fprintf(fid,'6 0 0 0 0 \n \n'); fprintf(fid,'%d \n',station); %number of station
for i=1:station
fprintf(fid,'%5.1f%8.1f%8.1f%4.0f%8.1f%8.1f \n',x(i)*10^-3,y(i)*10^-3,press(i),temp(i),dire(i),speed(i));
end
fprintf(fid,'\n');
%reads the utm coordinates
xlRange = 'H4:H4'; ut=xlsread(fullname1,xlRange); xlRange = 'I4:I4';
vt=xlsread(fullname1,xlRange); [tx,ty,tzone]=deg2utm(ut,vt); %makes utm conversion
%writes data to the created winds.dat file
fprintf(fid,'%3.0f. %4.0f.\n',tx*10^-3,ty*10^-3);
tsondeindx=round(gridx+((ut-corner2NS)*gridx)/(corner2NS-corner1NS));
%estimates the location of t-sonde point in terms of indices
tsondeindy=round(gridy+((vt-corner2EW)*gridy)/(corner2EW-corner1EW));
xlRange = 'K3:K30'; %reads pressure values changing with height (for the t-sonde point)
tpress = xlsread(fullname1,xlRange);
xlRange = 'L3:L30'; %reads heights for corresponding sigma values (for the t-sonde point)
theight = xlsread(fullname1,xlRange);
xlRange = 'M3:M30'; %reads pressure values changing with height (for the t-sonde point)
ttemp = xlsread(fullname1,xlRange)-273.1;
xlRange = 'N3:N30'; %reads u components of the velocity changing with height (for the t-sonde point)
tucomp = xlsread(fullname1,xlRange);
xlRange = 'O3:O30'; %reads v components of the velocity changing with height (for the t-sonde point)
tvcomp = xlsread(fullname1,xlRange);
tspeed=sqrt(tucomp.^2+tvcomp.^2); %calculates winds speed
tdir=180+atan2(tucomp,tvcomp)*(180/pi); %calculates wind direction
sigmas=length(tpress); %counts sigma levels
sigmas=4;
for i=1:sigmas
if (tdir(i) > 360)
tdir(i)= tdir(i)-360;
end
end
%writes data to the created winds.dat file
fprintf(fid,'%d \n',sigmas);
for j=1:sigmas
fprintf(fid,'%5.0f.%4.0f.%7.2f \n',theight(j),tdir(j),tspeed(j));
end
fprintf(fid,'\n\n%3.0f. %4.0f.\n',tx*10^-3,ty*10^-3); fprintf(fid,'%d 3\n',sigmas);
fprintf(fid,' z(m) T(C) p(mb) \n');
for k=1:sigmas
fprintf(fid,'%5.0f.%8.1f%10.1f \n',theight(k),ttemp(k),tpress(k));
end
fprintf(fid,'\n\nHt(m) (deg) (m/s)\n'); fprintf(fid,'%d \n',sigmas);
for j=1:sigmas
fprintf(fid,'%5.0f.%4.0f.%7.2f \n',theight(j),tdir(j),tspeed(j));
end
```

Figure A.4: wocss.m (cont.)

```
fprintf(fid,'%d ',date(1:4)); fprintf(fid,'\nEnd of the winds.dat file');
%terrain array is formed using the data from .dat filec
for i=1:gridx
for j=1:gridy
terrainarray(i,j)=terrain((i-1)*gridy+j);
end
end
for i=1:gridx
for j=1:gridy
if (j==1)
fprintf(fid3,'%3.0f',terrainarray(i,j));
else
fprintf(fid3,'%4.0f',terrainarray(i,j));
end
end
if(i<gridx)
fprintf(fid3,'\n');
end
end
%checks if the tsondeix is close to the edges
if(tsondeindx<5)
tsondeindx=5;
end
if(tsondeindx>gridx-5)
tsondeindx=gridx-5;
end
if(tsondeindy<5)
tsondeindy=5;
end
if(tsondeindy>gridy-5)
tsondeindy=gridy-5; end
%Here index of the 5 low points around the t-sonde point is determined
tsondeoriginal(1,1)=terrainarray(tsondeindx,tsondeindy); %original data is saved
terrainarray(tsondeindx,tsondeindy)=999; %t-sonde point is set to be 999m
%to make sure that the program don't find t-sonde point itself as a low point
%finds the indices of the low points arround the t-sonde point by searching
%within a small array with a size (9*9)
searchby=4;
for i=1:2*searchby+1
for j=1:2*searchby+1
terraintsonde(i,j)=terrainarray(tsondeindx-searchby+i-1 ,tsondeindy-searchby+j-1);
end
end
%5 low points are determined (indices are for the smallest array (9*9))
N=5;
[list,ix]=sort(terraintsonde(:)); [lowix, lowiy] = ind2sub( size(terraintsonde), ix(1:N) );
%indices are converted to their corresponding values in terrain array
for i=1:5
lowix(i)=lowix(i)+tsondeindx-searchby-1;
lowiy(i)=lowiy(i)+tsondeindy-searchby-1;
end
%t-sonde point's height is returned to its original value
terrainarray(tsondeindx,tsondeindy)=tsondeoriginal(1,1);
%writes data to the created run.dat file
fprintf(fid4,'**********************run.dat file*****************************\n');
fprintf(fid4,'1   * NSKIP ascii option writes every nskip grid pts in x & y. \n');
fprintf(fid4,'10  * NLVL:number of flow surfaces used for calculations. \n');
fprintf(fid4,'0.0,0.05,0.1,0.2,0.3,0.4,0.5,0.6,0.8,1.0 * SIGMA(NLVL):sigma values of flow levels. \n');
```

Figure A.4: wocss.m (cont.)

```
fprintf(fid4,'7 * NFLAT: # of horiz. sfcs for interpol. (includes anemom. lvl).\n');
fprintf(fid4,'10.,50.,100.,200.,400.,800.,1000. * zchooz: heights (m, msl) of horiz sfcs. \n');
fprintf(fid4,'200,1,1 * NUMNWS,NUMTMP,numdop: total # sta., # upper wind & t-sondes. \n');
if (conversion1==1)
fprintf(fid4,'1.0,');
else
fprintf(fid4,'0.515,');
end
if (conversion2==1)
fprintf(fid4,'1.0 * SPDCNV,HTCNV conv factors input spds to m/s and heights to m. \n');
else
fprintf(fid4,'0.3048 * SPDCNV,HTCNV conv factors input spds to m/s and heights to m.\n');
end
fprintf(fid4,'%d,%d * MCRS,NCRS: # rows/cols. \n',gridx,gridy);
fprintf(fid4,'%.2f * DSCRS:dx -- grid spacing (km). \n',gridsize);
fprintf(fid4,'%.1f,%.1f * UTMAPX,UTMAPY:utms of reference point. \n',corner1utmx,corner1utmy);
fprintf(fid4,'1,1  * kgridx,kgridy, indices of reference point. \n');
fprintf(fid4,'1500. * AVTHK -- ht (m) of top sfc over low point. \n');
fprintf(fid4,'1.0  * SLFAC slope fact 1st guess top sfc (0=flat,1=terr follow). \n');
fprintf(fid4,'0.2 * CMPRES max compress of space bet sfcs smaller=less rise. \n');
fprintf(fid4,'0.001 * DPOTMIN min. theta lapse rate (deg/m) -- low stab lim. \n');
fprintf(fid4,'0.05,10.0 * ZZERO,Z10 sfc roughness length (m) & anemometer ht. (m). \n');
fprintf(fid4,'0.1 * D2MIN: min. dist for interp. wts in grid units. \n');
fprintf(fid4,'2.0  * DTWT: distance weight power --wt=1/(Dist**DTWT). \n');
fprintf(fid4,'20 * NITer, iteration limit in subroutine bal5. \n');
fprintf(fid4,'0.2 * ADJMAX: max adj fact near obs 0=no adj & 1=reg adj. \n');
for i=1:5
fprintf(fid4,'%d,%d *indices of %dth low point. \n',lowix(i),lowiy(i),i);
end
fprintf(fid4,'1 * NEND number of cases before stopping. \n');
figure(1); contourf(terrainarray); colorbar; lowpoint=0; highpoint=999;
figure(2); surf(terrainarray); shading interp; view(2); caxis manual
caxis([lowpoint highpoint]); colorbar;
saveas(figure(1),[pwd '/canakkale/2010-2040/1st/topo900c.jpg']);
saveas(figure(2),[pwd '/canakkale/2010-2040/1st/topo900s.jpg']);

clear all;
```

Figure A.4: wocss.m (cont.)

APPENDIX B: EXCEL FILES

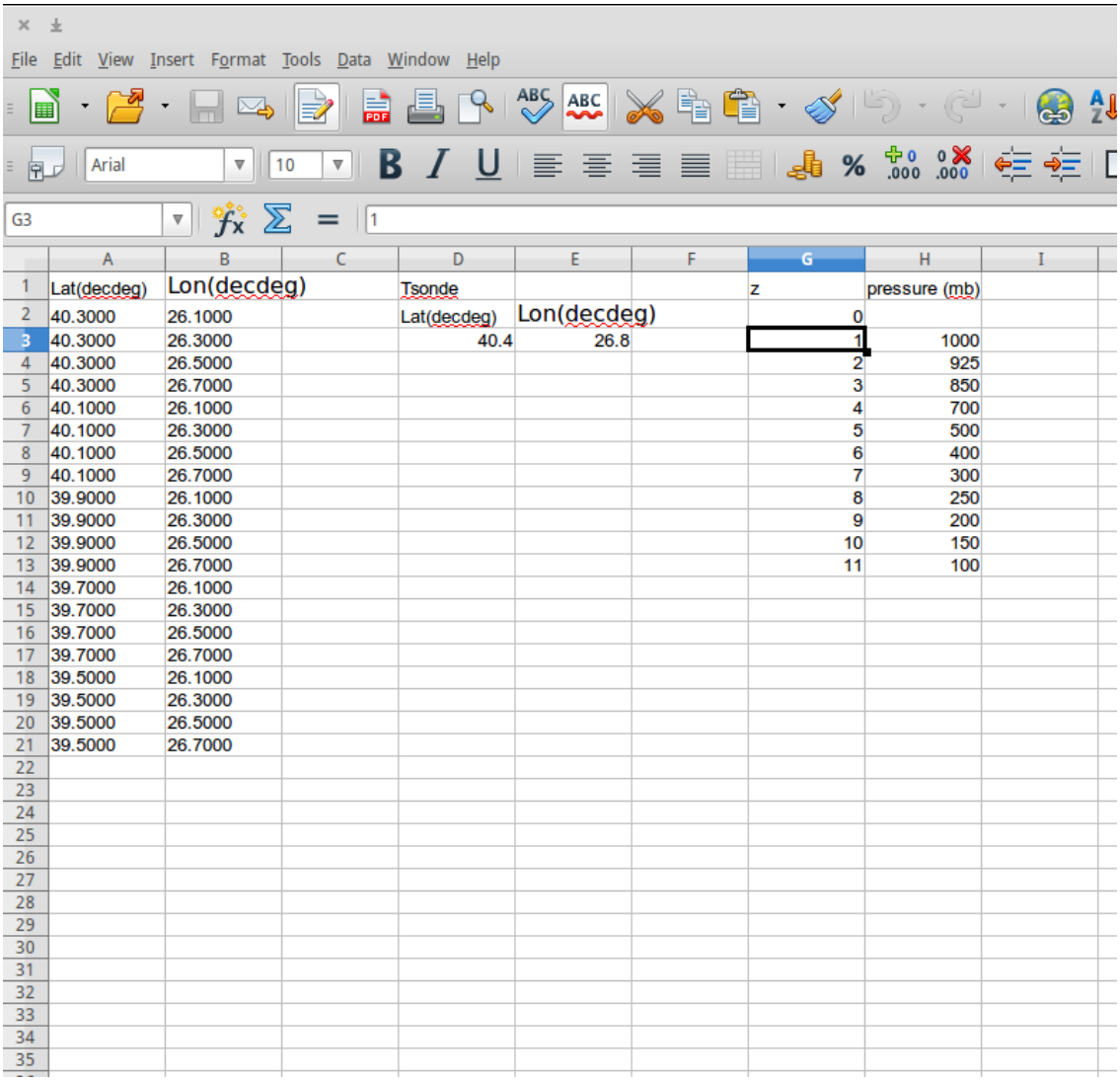

	A	B	C	D	E	F	G	H	I
1	Lat(decdeg)	Lon(decdeg)		Tsonde			z	pressure (mb)	
2	40.3000	26.1000		Lat(decdeg)	Lon(decdeg)		0		
3	40.3000	26.3000		40.4	26.8		1	1000	
4	40.3000	26.5000					2	925	
5	40.3000	26.7000					3	850	
6	40.1000	26.1000					4	700	
7	40.1000	26.3000					5	500	
8	40.1000	26.5000					6	400	
9	40.1000	26.7000					7	300	
10	39.9000	26.1000					8	250	
11	39.9000	26.3000					9	200	
12	39.9000	26.5000					10	150	
13	39.9000	26.7000					11	100	
14	39.7000	26.1000							
15	39.7000	26.3000							
16	39.7000	26.5000							
17	39.7000	26.7000							
18	39.5000	26.1000							
19	39.5000	26.3000							
20	39.5000	26.5000							
21	39.5000	26.7000							
22									
23									
24									
25									
26									
27									
28									
29									
30									
31									
32									
33									
34									
35									

Figure B.1: coordinates.xlsx

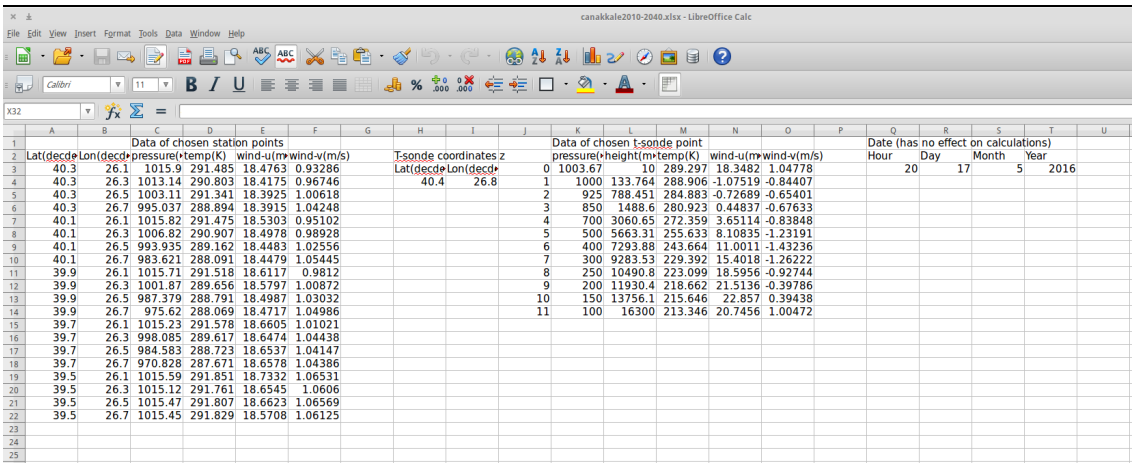

	A	B	C	D	E	F	G	H	I	J	K	L	M	N	O	P	Q	R	S	T	U
1			Data of chosen station points								Data of chosen t-sonde point						Date (has no effect on calculations)				
2	Lat(decd	Lon(decd	pressure(	temp(K)	wind-u(m	wind-v(m/s)		T-sonde coordinates z			pressure(	height(m	temp(K)	wind-u(m	wind-v(m/s)		Hour	Day	Month	Year	
3	40.3	26.1	1015.9	291.485	18.4763	0.93286		Lat(decd	Lon(decd	0	1003.67	10	289.297	18.3482	1.04778		20	17	5	2016	
4	40.3	26.3	1013.14	290.803	18.4175	0.96746		40.4	26.8	1	1000	133.764	288.906	-1.07519	-0.84407						
5	40.3	26.5	1003.11	291.341	18.3925	1.00618				2	925	788.451	284.883	-0.72689	-0.65401						
6	40.3	26.7	995.037	288.894	18.3915	1.04248				3	850	1488.6	280.923	0.44837	-0.67633						
7	40.1	26.1	1015.82	291.475	18.5303	0.95102				4	700	3060.65	272.359	3.65114	-0.83848						
8	40.1	26.3	1006.82	290.907	18.4978	0.98928				5	500	5663.31	255.633	8.10835	-1.23191						
9	40.1	26.5	993.935	289.162	18.4483	1.02556				6	400	7293.88	243.664	11.0011	-1.43236						
10	40.1	26.7	983.621	288.091	18.4479	1.05445				7	300	9283.53	229.392	15.4018	-1.26222						
11	39.9	26.1	1015.71	291.518	18.6117	0.9812				8	250	10490.8	223.099	18.5956	-0.92744						
12	39.9	26.3	1001.87	289.656	18.5797	1.00872				9	200	11930.4	218.662	21.5136	-0.39786						
13	39.9	26.5	987.379	288.791	18.4987	1.03032				10	150	13756.1	215.646	22.857	0.39438						
14	39.9	26.7	975.62	288.069	18.4717	1.04986				11	100	16300	213.346	20.7456	1.00472						
15	39.7	26.1	1015.23	291.578	18.6605	1.01021															
16	39.7	26.3	998.085	289.617	18.6474	1.04438															
17	39.7	26.5	984.583	288.723	18.6537	1.04147															
18	39.7	26.7	970.828	287.671	18.6578	1.04386															
19	39.5	26.1	1015.59	291.851	18.7332	1.06531															
20	39.5	26.3	1015.12	291.761	18.6545	1.0606															
21	39.5	26.5	1015.47	291.807	18.6623	1.06569															
22	39.5	26.7	1015.45	291.829	18.5708	1.06125															
23																					
24																					
25																					

Figure B.2: canakkale2010-2040.xlsx

APPENDIX C: WOCSS FILES

```
**********run.dat file*****************************
1   * NSKIP ascii option writes every nskip grid pts in x & y.
10  * NLVL:number of flow surfaces used for calculations.
0.0,0.05,0.1,0.2,0.3,0.4,0.5,0.6,0.8,1.0 * SIGMA(NLVL):sigma values of flow levels.
7 * NFLAT: # of horiz. sfcs for interpol. (includes anemom. lvl).
10.,50.,100.,200.,400.,800.,1000. * zchooz: heights (m, msl) of horiz sfcs.
200,1,1 * NUMNWS,NUMTMP,numdop: total # sta., # upper wind & t-sondes.
1.0,1.0 * SPDCNV,HTCNV conv factors input spds to m/s and heights to m.
108,108 * MCRS,NCRS: # rows/cols.
0.99 * DSCRS:dx -- grid spacing (km).
414.0,4372.7 * UTMAPX,UTMAPY:utms of reference point.
1,1  * kgridx,kgridy, indices of reference point.
1500. * AVTHK -- ht (m) of top sfc over low point.
1.0  * SLFAC slope fact 1st guess top sfc (0=flat,1=terr follow).
0.2 * CMPRES max compress of space bet sfcs smaller=less rise.
0.001 * DPOTMIN min. theta lapse rate (deg/m) -- low stab lim.
0.05,10.0 * ZZERO,Z10 sfc roughness length (m) & anemometer ht. (m).
0.1 * D2MIN: min. dist for interp. wts in grid units.
2.0  * DTWT: distance weight power --wt=1/(Dist**DTWT).
20 * NITer, iteration limit in subroutine bal5.
0.2 * ADJMAX: max adj fact near obs 0=no adj & 1=reg adj.
100,92 *indices of 1th low point.
101,92 *indices of 2th low point.
102,92 *indices of 3th low point.
103,92 *indices of 4th low point.
104,92 *indices of 5th low point.
1 * NEND number of cases before stopping.
```

Figure C.1: rundat.dat

```
20 17 5 2016

6 0 0 0 0

6 0 0 0 0

20
423.5  4461.4  1015.9  18   267.1    18.5
440.5  4461.3  1013.1  18   267.0    18.4
457.5  4461.2  1003.1  18   266.9    18.4
474.5  4461.1   995.0  16   266.8    18.4
423.3  4439.2  1015.8  18   267.1    18.6
440.3  4439.1  1006.8  18   266.9    18.5
457.4  4439.0   993.9  16   266.8    18.5
474.4  4438.9   983.6  15   266.7    18.5
423.1  4417.0  1015.7  18   267.0    18.6
440.2  4416.9  1001.9  17   266.9    18.6
457.3  4416.8   987.4  16   266.8    18.5
474.4  4416.7   975.6  15   266.7    18.5
422.8  4394.8  1015.2  18   266.9    18.7
440.0  4394.7   998.1  17   266.8    18.7
457.1  4394.6   984.6  16   266.8    18.7
474.3  4394.5   970.8  15   266.8    18.7
422.6  4372.7  1015.6  19   266.7    18.8
439.8  4372.5  1015.1  19   266.7    18.7
457.0  4372.4  1015.5  19   266.7    18.7
474.2  4372.3  1015.5  19   266.7    18.6

483. 4472.
4
   10. 267.  18.38
  134.  52.   1.37
  788.  48.   0.98
 1489. 326.   0.81


483. 4472.
4 3
 z(m) T(C) p(mb)
   10.    16.2    1003.7
  134.    15.8    1000.0
  788.    11.8     925.0
 1489.     7.8     850.0


Ht(m) (deg) (m/s)
4
   10. 267.  18.38
  134.  52.   1.37
  788.  48.   0.98
 1489. 326.   0.81
20 17 5 2016
End of the winds.dat file
```

Figure C.2: winds.dat